A multimodal platform for neuropathological studies of Alzheimer's disease and related neurodegenerative disorders

John F. Crary, MD-PhD[1,2,3,4,5], Dushyant Purohit, MD[1,2,3,4,5,11], MD, Marco Hefti, MD, Maxim Signaevsky, MD-PhD[1,2,3,4,5], Susan Morgello, MD[1,2,3,7], Ann C. McKee, MD[8,9], Julie A. Schneider, MD[10], Mary C. Sano, PhD[4,5,6,11]

1. Department of Pathology, 2. Neuroscience, 3. Friedman Brain Institute, 4. Alzheimer's Disease Research Center, 5. Ronald M. Loeb Center for Alzheimer's Disease and 6. Department of Psychiatry, 7. Department of Neurology, Icahn School of Medicine at Mount Sinai, New York, NY, 10029, 8. Department of Neurology, Pathology, Alzheimer's Disease Center, CTE Program, Boston University School of Medicine, 72 East Concord Street, Boston, MA 02118, 9. VA Boston Healthcare System, 150 South Huntington Avenue, Boston 02130, MA, 10. Departments of Pathology (Neuropathology) and Neurological Sciences, Rush University Medical Center, Chicago IL 60612, USA, 11. James J Peters VAMC, Bronx, NY.

Abstract

Alzheimer's disease (AD) remains a public health crisis. However, there is an alarming shortage of neuropathologists that are necessary to meet the objectives of the National Plan to Address Alzheimer's Disease. The goal of this award is to advance the career development of Dr. John F. Crary, and position him to serve as an AD Research Center (ADRC) neuropathology (NP) core leader. Under the mentorship of Dr. Sano and the Mount Sinai ADRC leadership, Dr. Crary underwent training with the goals of developing 1. the competence to collect and deploy human brain tissue for research, 2. an aptitude for innovating through novel neuropathological concepts, and 3. the ability to educate trainees. In addition, Dr. Crary visited the Rush and Boston University NP cores. Dr. Crary also received additional mentorship from the Manhattan HIV brain bank leadership. To achieve these goals, Dr. Crary launched a new autopsy series focusing on AD-related cognitive disorders (i.e., a-synucleinopathies and tauopathies). Dr. Crary initiated collaborations with neurologists, secured a new IRB protocol, deployed a revised anatomical gift consent, developed a new rapid tissue parcellation/freezing protocol, and created a new database/inventory management system. Dr. Crary expanded his research program by developing a large multi-institutional collaboration to validate the neuropathological criteria for PART highlighting that this pathology is an independent correlate of dementia, and presented this work at the ADC NP core directors meeting. Finally, Dr. Crary is mentoring four neuropathology fellows. Together, these activities have greatly contributed to Dr. Crary's goal of succeeding as an NP core leader.

Aim 1. To develop proficiency in managing and maintaining a large dementia brain biorepository

A. On site training at Rush University (Dr. Schneider), Boston University (Dr. McKee), and Mount Sinai (Drs. Dushyant Purohit & Susan Morgello)

B. A new longitudinal genetics and biomarker study in neurodegenerative cognitive & movement disorders at Mount Sinai (in collaboration with Steven Frucht, MD, Ritesh Rhamdani, MD, Ruth Walker, MD, and Towfique Raj, PhD)

Table 1. Frontotemporal dementia, atypical parkinsonism and Lewy body disease cohort

	Total		Anatomical gift		
	n	(M/F)	n	(M/F)	%
Lewy body disease and Parkinson disease	124	(87/37)	22	(12/10)	18%
Atypical parkinsonism and FTLD	12	(6/6)	6	(4/2)	50%
Control	36	(14/22)	2	(1/1)	6%
Other*	14	(7/7)	2	(2/0)	14%
Total	186	(113/73)	32	(19/13)	17%

*X-linked parkinsonism, cerebellar ataxia, Wilson's disease, dystonia, Huntington's disease, myoclonus-dystonia, Bell's palsy/Grave's disease, Alzheimer's disease

C. A novel high throughput brain banking protocol (Drs. Purohit, Hefti and Signaevsky)

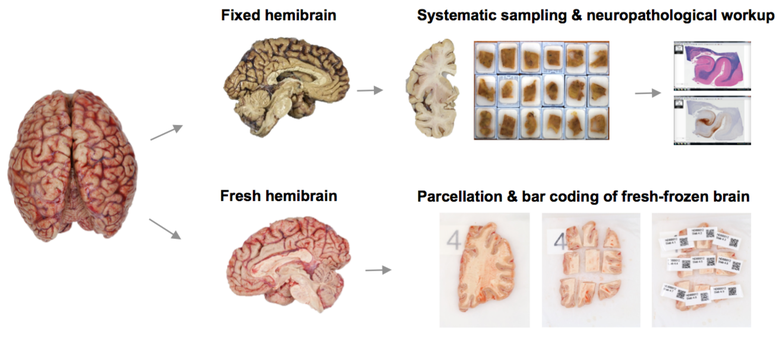

Figure 1. A novel efficient rapid brain banking parcellation and barcoding protocol. Brain and brainstem specimens are bisected, with half being processed fresh and the other fixed in 10% neutral buffered formalin with extensive systematic sampling and IHC. The fresh half is bread loafed, dissected, barcoded and frozen using liquid nitrogen vapors to preserve morphology. Data is stored using an implementation of the NACC NP forms in Redcap. Current n=34, the goal is 300 over the next three years!

Aim 2. To validate the neuropathological criteria for primary age-related tauopathy

A. Clinicopathological studies of PART in the National Alzheimer's Disease Coordinating Center Database (in collaboration with L. Besser, C. Mock and W. Kukall)

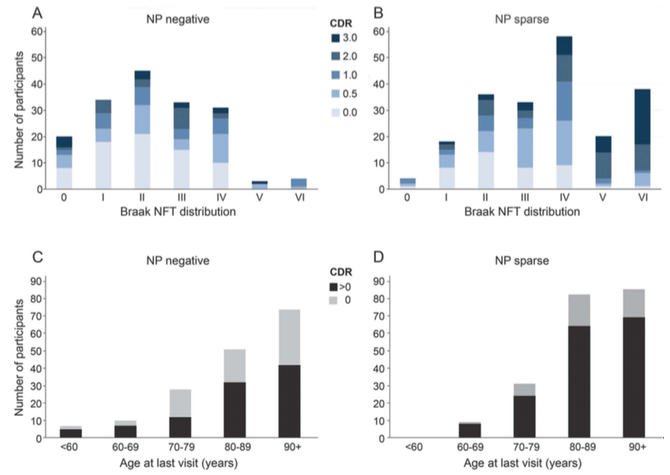

Figure 2. NFT stage and age by CDR and NP scores in PART. The sample consisted of 98 symptomatic PART-definite, 72 asymptomatic PART-definite, 165 symptomatic amyloid sparse (AS), and 42 asymptomatic AS participants. PART-definite participants were less often symptomatic (58%) than AS participants (80%) (x2 p , 0.001). Although the majority of the PART-definite and AS participants had a CDR score ≤ 1, more of the AS group (39.1%) had a CDR score .1 than the PART-definite group (18.2%) (A and B). Only 4.1% of the PART-definite group had Braak stage V to VI, compared to 28.0% of the AS group (x2 p , 0.001) (A and B). There was no change in the proportion who were symptomatic with increasing age in the PART-definite and AS groups (C and D).

Table 2. Adjusted odds of symptomatic primary age-related tauopathy (*n*=377)

	PART, definite			Amyloid sparse		
Test	**OR**	**95% CI**	**p-value**	**OR**	**95% CI**	**p-value**
Age at last visit (years)	0.97	0.93-1.00	0.07	1.07	0.97-1.17	0.17
Education (years)	1.01	0.89-1.16	0.84	0.8	0.65-0.99	0.04
Depression	4.2	2.15-8.19	<0.0001	6.04	0.60-60.84	0.13
APOE (at least one ε4 vs no ε4 allele)	2.38	0.99-5.76	0.05	2.24	0.40-12.50	0.36
History of stroke (yes vs no)	8.09	2.63-24.82	0.0003	1.38	0.44-4.32	0.58
History of diabetes (yes vs no)	0.44	0.13-1.55	0.2	2.63	0.59-11.67	0.2
Braak stage (0 through VI)	1.42	1.04-1.95	0.03	1.91	1.07-3.43	0.03
Diffuse plaques (yes vs no)	0.49	0.22-1.07	0.07	0.32	0.02-5.55	0.44
Microinfarct (yes vs no)	1.38	0.61-3.11	0.44	1.88	0.44-8.05	0.39
Amyloid angiopathy (yes vs no)	1.39	0.54-3.53	0.49	2.75	1.14-6.64	0.02

Abbreviations: PART= primary age-related tauopathy; OR = odds ratio; CI = confidence interval; *APOE* = apolipoprotein E

B. The PART working group collaboration: Genetic and biochemical studies of tau and APP metabolites (sAPPα/β, Aβ) in aging and PART

Table 3. Primary age-related tauopathy working group

Institution or center	Collaborator(s)
Northwestern University	Eileen H. Bigio
Newcastle University	Johannes Attems
Emory University	Marla Gearing
Banner Sun Health Research Institute	Thomas G. Beach
University of Kentucky	Peter T. Nelson
University of Pennsylvania	John Q. Trojanowski & Edward Lee
University of Washington	Thomas J. Montine & C.D. Keene
Medical University of Vienna	Gabor G. Kovacs
University of Pittsburgh Medical Center	Julia Kofler
Oregon Health Science University	Randall L. Woltjer
University of Texas Southwestern	Charles L. White 3rd, Jamie Walker
University California Irvine	Claudia Kawas & Maria Corrada
Rush University	Julie A. Schneider
Washington University Saint Louis	Nigel J. Cairns
Columbia University	Jean Paul Vonsattel, Etty Cortez & Andrew Teich
Boston University	Ann C. McKee & Thor D. Stein
Mayo Clinic	Dennis W. Dickson & Melissa Murray
Icahn School of Medicine at Mount Sinai	Dushyant Purohit
University of California San Diego	Robert Rissman & Lawrence Hansen

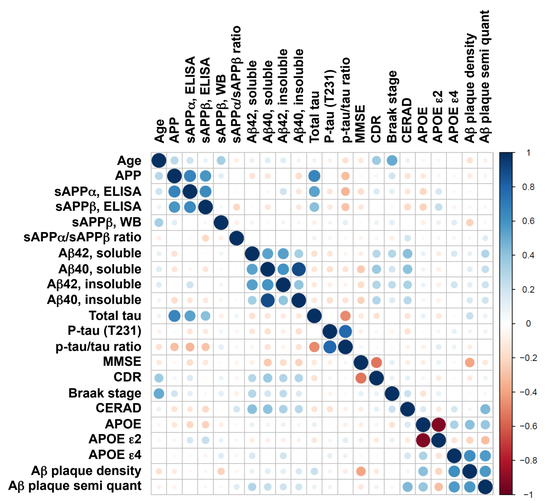

Figure 3. Clinical, neuropathological, genetic, and biochemical correlations in PART. Clinical data were provided by the contributing institution. APP, sAPP, Aβ 42/40, tau, p-tau, were measured using ELISA or Western blot, Pearson correlations were generated using GG plot in R Studio.

Aim 3. To broaden neuropathology education and train the next generation of neuropathologists

Table 5. Trainees

Name	Current position	Current project	Funding	Period
Neuropathology fellows				
Marco Hefti, MD	University of Iowa, Assistant prof., tenure track	Tau in brain development	K32 pending	2015-2017
Maxim Signaevsky, MD-PhD	Mount Sinai, Brain bank fellow	Tau pathology in CTE	ADRC NP award	2017–present
Jamie Walker, MD-PhD (co-mentor)	Northwestern, Brain bank fellow	Tau pathology in PART	ADRC NP award	2017–present
Shahram Saberi, MD	Mount Sinai, AP/NP resident	Molecular pathology of PSP/CBD		2017-present
Post-doctoral fellows				
Ismael Santa-Maria, PhD	Columbia University, Assistant professor, tenure track	Regulation of tau expression	R01	2010-2015
Bidisha Roy, PhD	Post-doctoral fellow	MicroRNA regulation of MAPT		2015-present
Kurt Farrell, PhD	Post-doctoral fellow	Genetic determinants of PART	F32	2016-present
Masters of Science in Biomedical Science students				
Jonathan Kofi Vordzorgbe	MS student	APP processing in aging		2016-present
Natalia Han	MS student	Quantificaiton of tau pathology		2017-present

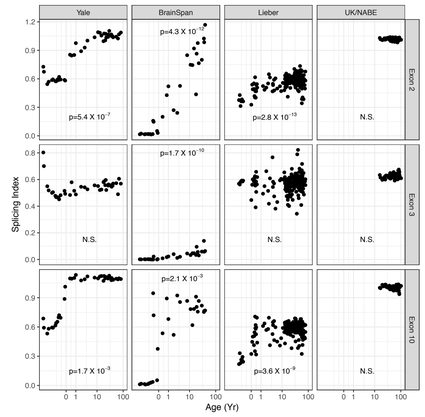

Figure 4. MAPT exons 2 and 10 show a rapid perinatal increase in splicing in multiple datasets. p-values calculated using generalized linear models including available covariates within each dataset (Yale = age, sex, RIN; BrainSpan = age, sex; Lieber = age, sex, RIN, race; UK/NABE = age, sex, RIN).

Future directions

1. **Continue to expand our post-mortem brain collection through increased collaboration with neurologists in the Mount Sinai Center for Cognitive Health and Movement Disorders, with a focus on atypical dementias**
2. **Continue neuropathological, biomarker and genetic studies of primary age-related tauopathy and other tauopathies**
3. **Continue to seek out training opportunities and support the career development of the next-generation of neuropathologists**
4. **Continue to advocate for the critical nature of neuropathological studies in aging and dementia research**

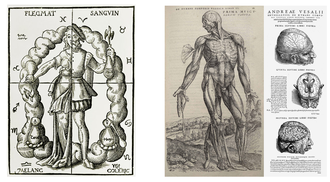

References and acknowledgments

1. Besser LM, Crary JF, Mock C, Kukull WA. Comparison of symptomatic and asymptomatic persons with primary age-related tauopathy. Neurology. 2017. doi: 10.1212/WNL.0000000000004521. PubMed PMID: 28916532.
2. McKee AC, Cairns NJ, Dickson DW, Folkerth RD, Keene CD, Litvan I, Perl DP, Stein TD, Vonsattel JP, Stewart W, Tripodis Y, Crary JF, Bieniek KF, Dams-O'Connor K, Alvarez VE, Gordon WA, group TC. The first NINDS/NIBIB consensus meeting to define neuropathological criteria for the diagnosis of chronic traumatic encephalopathy. Acta neuropathologica. 2016;131(1):75-86. Epub 2015/12/17. doi: 10.1007/s00401-015-1515-z. PubMed PMID: 26667418; PMCID: 4698281.
3. Crary JF. Primary age-related tauopathy and the amyloid cascade hypothesis: the exception that proves the rule? J Neurol Neuromedicine. 2016;1(6):53-7. PubMed PMID: 27819070; PMCID: PMC5094182.
4. Kang, H. J. et al. Spatio-temporal transcriptome of the human brain. Nature 478, 483-489, doi:10.1038/nature10523 (2011).
5. Lipska, B. K. et al. Critical factors in gene expression in postmortem human brain: Focus on studies in schizophrenia. Biological psychiatry 60, 650-658, doi:10.1016/j.biopsych.2006.06.019 (2006).
6. Colantuoni, C. et al. Temporal dynamics and genetic control of transcription in the human prefrontal cortex. Nature 478, 519-523, doi:10.1038/nature10524 (2011).
7. Ramasamy, A. et al. Genetic variability in the regulation of gene expression in ten regions of the human brain. Nature neuroscience 17, 1418-1428, doi:10.1038/nn.3801 (2014).

This work was supported by the National Institutes of Health grants [P50AG005138 (Sano), R01AG054008, R01NS095252], the Alzheimer's Association (NIRG-15-363188), the United States Department of Defense (13267017), and the Tau Consortium.

Using High-Throughput Omics Technologies on Formalin Fixed Paraffin Embedded Tissue

Eleanor Drummond[1], Shruti Nayak[1], Arline Faustin[1], Geoffrey Pires[1], Richard Hickman[1], Jiri Safar[2], Manor Askenazi[1], Mark Cohen[2], Tracy Haldiman[2], Chae Kim[2], Beatrix Ueberheide[1] and Thomas Wisniewski[1]

[1]New York University School of Medicine, New York, NY, USA, [2]Case Western Reserve University, Cleveland, OH, USA

Introduction

- **Rapidly progressive Alzheimer's disease (rpAD) is a particularly aggressive form of AD, with a median survival time of 7-10 months after diagnosis.**
- **To understand the biological mechanisms that underlie the rapid development of pathology in rpAD, localized proteomics (LC-MS/MS) was performed on amyloid plaques microdissected from rpAD and sAD patients and protein expression differences were quantified.**
- **We found significant differences in protein composition between rpAD and sAD plaques.**
- **Protein differences in rpAD plaques suggested that pathology was mediated by different mechanisms and highlighted the potential importance of synaptic dysfunction in the accelerated development of plaque pathology in rpAD.**

Background

FFPE blocks
0.5-8 years
archival time

The vast majority of human tissue specimens are formalin-fixed, paraffin embedded (FFPE) archival tissue

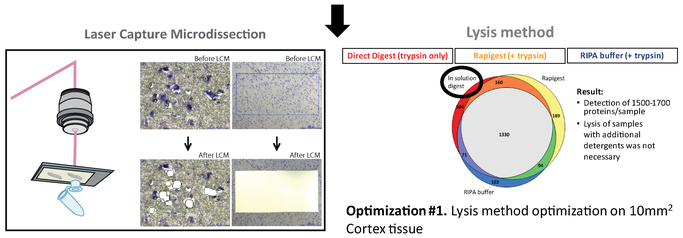

Optimization #1. Lysis method optimization on 10mm^2 Cortex tissue

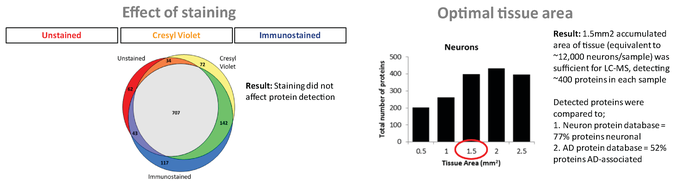

Optimization #2. Staining method optimization on 10mm2 Cortex tissue

Optimization #3. Minimum number of neurons necessary

Methods

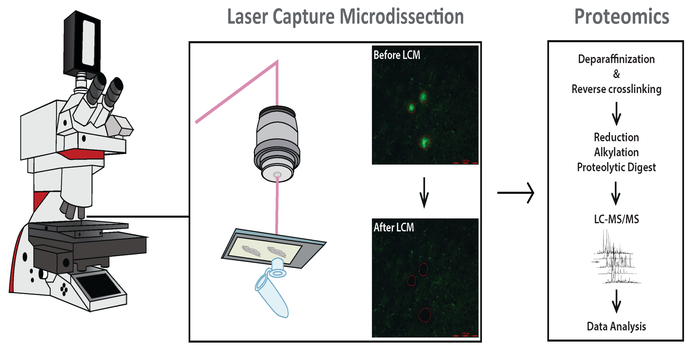

Results

	rpAD	sAD
Number of cases	22 (12 Female / 10 Male)	22 (15 Female / 7 Male)
Average age (±SEM)	70.0 (±2.2) years	80.1 (±1.9) years
Tissue archival time (±SEM)	6.0 (±0.22) years	4.7 (±0.5) years
Disease duration (±SEM)	9.2 (±1.3) months	122 (±8.0) months
Postmortem interval	45.1 (±7.7) h	31.1 (±7.4) h
Predominant plaque type microdissected	6 neuritic / 5 diffuse / 11 mixed	3 neuritic / 5 diffuse / 14 mixed
Number of plaques microdissected (±SEM)	733 (±52)	751 (±49)
Average size of plaques microdissected (±SEM)	3099 (±213) µm^2	2958 (±220) µm^2
Average number of proteins identified using LC-MS (±SEM)	941 (±37)	884 (±47)

Table 1 : **General patient and microdissected plaque characteristics.**

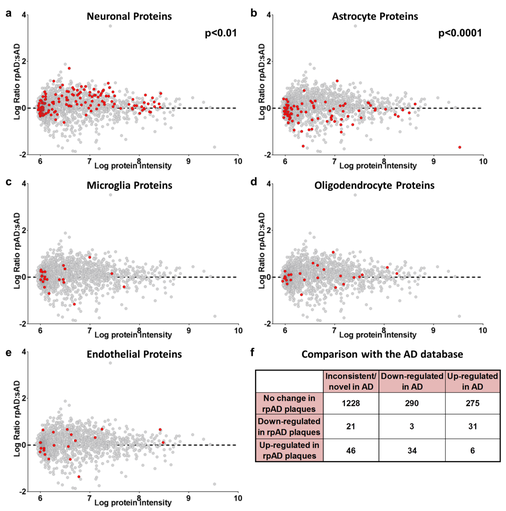

	Inconsistent/ novel in AD	Down-regulated in AD	Up-regulated in AD
No change in rpAD plaques	1228	290	275
Down-regulated in rpAD plaques	21	3	31
Up-regulated in rpAD plaques	46	34	6

Fig.2: **Cell type-specific protein expression differences in rpAD plaques**. All proteins highlighted in red correspond to neuronal proteins (**a**) astrocyte proteins (**b**) microglial proteins (**c**) oligodendrocyte proteins (**d**) and (**e**) endothelial cell proteins. (**f**) Fisher's exact test was used to determine significance.

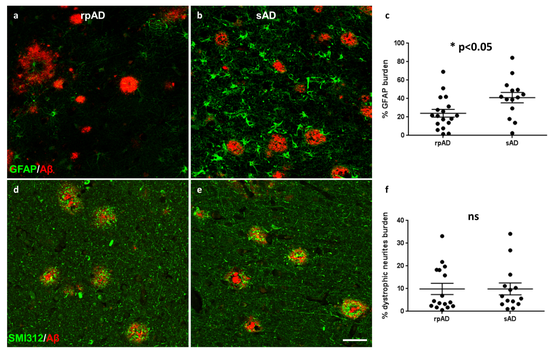

Fig.3: **Altered levels of plaque associated astrocytes (a,b,c), but not plaque-associated dystrophic neurites (d,e,f) in rpAD**. Significance was determined using an unpaired *t* test (rpAD *n* = 18) and (sAD *n* = 14); data show mean ± SEM.

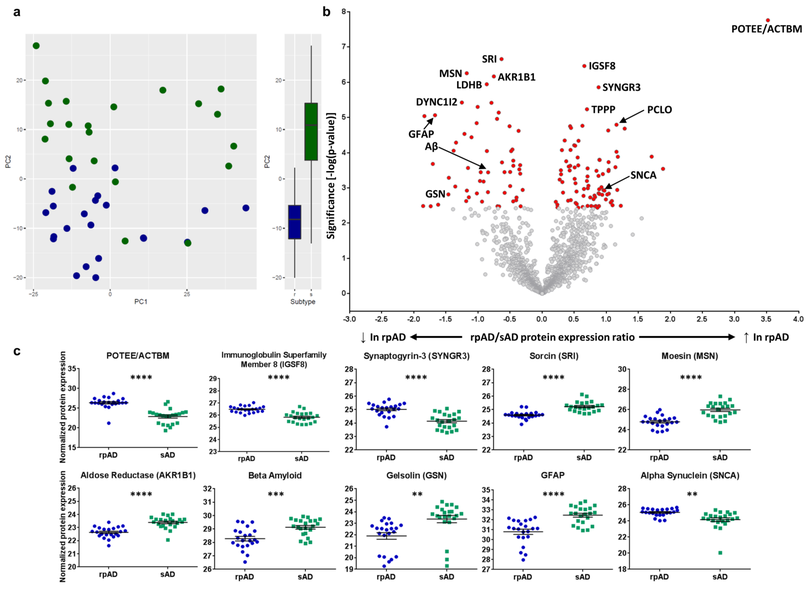

Fig.1: **Differences in the rpAD and sAD plaque proteome**. **a** Principal component analysis . **b** Volcano plot showing protein expression differences of all proteins identified in plaques. Significance was determined using a two-sided Welch's *t* test and Benjamini–Hochberg False Discovery Rate (FDR) set to 5%. **c** Proteins of interest with significantly altered levels in rpAD plaques. Significance was determined using an unpaired *t* test with Welch's correction. Data show mean ± SEM; ****$p < 0.0001$; ***$p < 0.001$; **$p < 0.01$.

Conclusions

- **Most comprehensive analysis of protein composition in amyloid plaques to date**
- **Presence of Secernin-1, a novel amyloid-associated protein, was confirmed using standard IHC methods**
- **rpAD and sAD plaques have significantly different protein composition;**
  - **141 proteins had significantly altered expression in rpAD plaques**
  - **rpAD plaques contain more neuronal proteins**
  - **sAD plaques contain more astrocyte proteins**
- **Future targeted studies examining the role of these altered proteins in AD could help determine the mechanism that underlies the rate of disease progression in AD and the causal factors involved in the development of amyloid plaques.**

References

- Eleanor Drummond, Shruti Nayak, Beatrix Ueberheide and Thomas Wisniewski (2015) Proteomic analysis of neurons microdissected from formalinfixed, paraffin-embedded Alzheimer's disease brain tissue. *Scientific Reports.* doi:10.1038/srep15456
- Eleanor Drummond, Shruti Nayak, Arline Faustin, Geoffrey Pires, Richard Hickman, Jiri Safar, Manor Askenazi, Mark Cohen, Tracy Haldiman, Chae Kim, Beatrix Ueberheide and Thomas Wisniewski (2017) Proteomic differences in amyloid plaques of rapidly progressive Alzheimer's disease and sporadic Alzheimer's disease. Acta neuropathol. doi:10.1007/ doi:10.1007/ s00401-017-1691-0

Acknowledgments

- Patients' families
- The CJD Foundation
- Members of the National Prion Disease Pathology Surveillance Center

Support from the following Grants:

- NS074317
- u51 CK000309
- AG08051
- AG20245
- NS073502
- The Spitz Family Foundation

Working towards the application of new imaging technologies in Alzheimer's Disease and dementia research settings

Margaret E. Flanagan[1], Kausalia Vijayaragavan[2], Sean Bendall[2], Michael Angelo[2], Laura S. Hemmy[3], Dennis Ai[4], Greg Kovacs[4],, Kathleen S. Montine[2] Thomas J. Montine[2]

1. University of Minnesota, Department of Laboratory Medicine and Pathology, Minneapolis, MN
2. Stanford University, Department of Pathology. Stanford, CA
3. University of Minnesota Department of Psychiatry, Minneapolis, MN
4.SRI International, Menlo Park, CA.

Abstract

- Alzheimer's disease center (ADC) researchers are working to translate research advances into improved diagnosis and care for individuals with AD.
- The Neuropathology Core is an essential component of the ADC:
  - Post-mortem verification of the diagnosis of AD (autopsy remains gold standard) with tissue banking playing an important role in supporting translational research.
  - Necessary for applying novel technologies, techniques and/or information to increase the value of stored tissues and fluids.
- Improvised and worked with developing new quantitative multiplexing technologies to be used in in neurodegenerative research settings due to funding restrictions prohibiting my original research project plan.
- This training supplement has enabled me to explore different multiplexing platforms, form invaluable research collaborations for the future and set me up to continue my research at my new faculty position.

Introduction

- Many ADCs have expressed a strong need for career development for neuropathologists in hopes of recruiting strong candidates.
  - Provide exposure and training necessary to lead a Neuropathology Core
- Worked with different new technologies this year that allow for simultaneous imaging of numerous proteins that mark subtypes of neuronal bodies, synapses, non-neuronal cell types, regulatory signaling markers, neuroinflammatory markers and products of AD risk genes:
  - Mutiplexed ion beam imaging (MIBI) with the Montine, Bendall and Angelo laboratories including helping develop AD & PD panels.
    - MIBI previously used on formalin fixed paraffin embedded breast tumor samples[1]
  - Hyperspectral immunofluorescence microscopy in collaboration with SRI International
- This training supplement has enabled me to explore different multiplexing platforms, form invaluable research collaborations for the future:
  - Helped me obtain my new faculty position where I have the opportunity to continue working with quantitative multiplexing technologies to further study longitudinal community based cohorts to better understand neurodegenerative disease mechanisms and protein interactions.

Methods & Materials

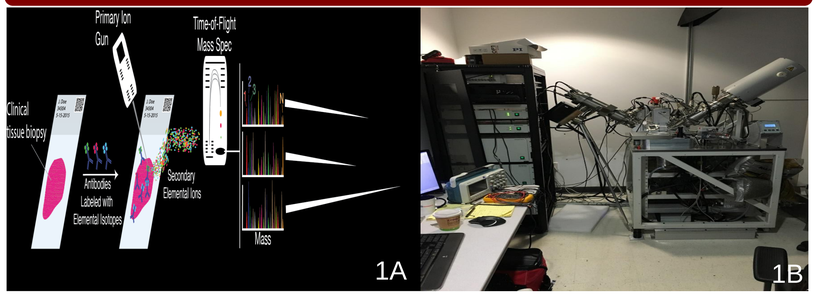

Figure 1: A) MIBI work flow B) Alpha model of MIBI at Stanford University

Results

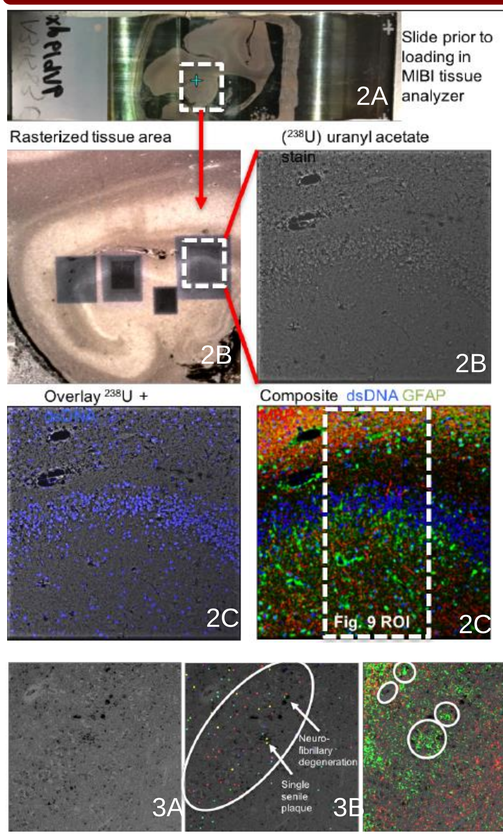

Figure 2: A) Archival brain tissue (5 microns thick). B) Slide of post-MIBI scanned section with enlargement of scanned area showing MIBI image from uranyl channel. C) Overlay with dsDNA for nuclear factors and composite 3-color image probing for astrocytes (GFAP) and neuronal axons (MBP: orange). FOV= 800 x 800 micrometers.

Figure 3: A) MIBI image from silver channel on slide previously stained with Gallyas 107 Ag+ stain. B) Overlay of Ag+ channel with 6 known protein products of AD associated genes (key below). C) Ellipses show co-localization of AD risk factors and GFAP (green) to Ag+ areas. MBP is also shown in red. FOV= 800 x 800 micrometers.

Figure 3B color key:

- ApoE: blue
- A β: yellow
- αsyn: green
- CD33: cyan
- CD35/CR1: red

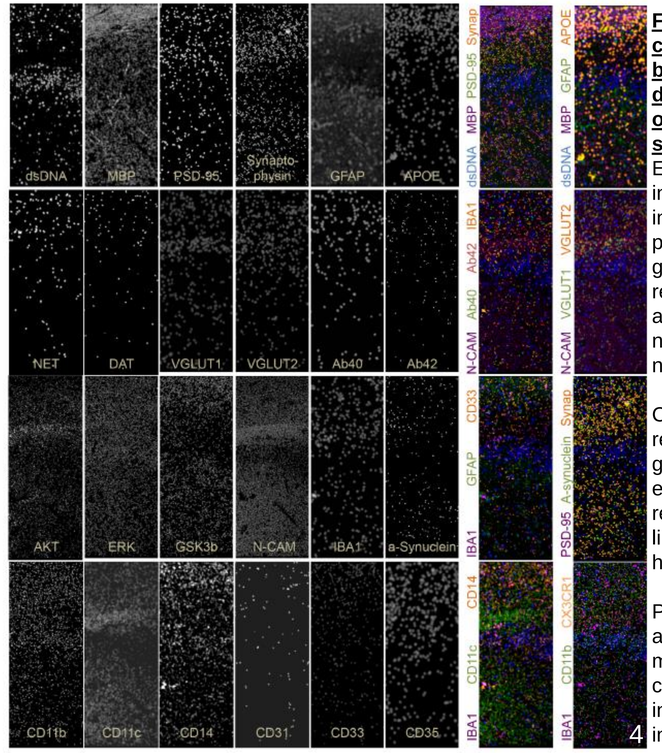

Figure 4: Proof of concept in human brain tissue demonstrating 24 of the 32 plex MIBI scan.
Expression of individual markers: including structural proteins, AD risk gene products, regulatory proteins and surrogates for neuronal and non-neuronal lineages.

Composite images reveal AD associated gene products expression patterns relative to respective lineage marker and hippocampal layer.

Produces large amount of data that machine learning can used to help interpret the information.

Conclusions & Future Directions

- R01 MIBI collaboration: Studying resilience in Nun Study cohort based at UMN
- SRI collaboration: multiplexed hyperspectral immunofluorescence; still in the development stages.
- Future plans to work with immunofluorescence/oligonucleotide based multiplexing platform (CODEX).[2]
- Applying for Minnesota collaborative grant with Dezhi Liao and Michael Koob (UMN) and Michelle Mielke (Mayo Clinic): **Targeting tau phosphorylation and missorting to treat Alzheimer's disease**
- Assistant professor position at UMN where I am part of the Grossman Center For Memory Research and Care. We are working hard to apply for a national ADC where I hope to one day become the core leader of the Neuropathology and Biospecimens Core.

References

1. Angelo M, et al. Multiplexed ion beam imaging of human breast tumors. Nat. Med. 2014;20:436–442. doi: 10.1038/nm.3488.
2. Kennedy-Darling et al. Multiparametic immunofluorescence analysis of the tumor microenvironment using CODEX. Cancer Immunology Research: Translating Science into Survival. Nov. 2016:4(11)

RNAseq in frontal cortex of young subjects with ApoE 3/3 and 3/4 genotypes free of Alzheimer's pathology

Andrew R. Guajardo MD, Gay Rudow BA, Olga Pletnikova MD, Dan Arking PhD, Juan C. Troncoso MD
Division of Neuropathology, Alzheimer Disease Research Center, The Johns Hopkins University School of Medicine

ABSTRACT

Background: The apolipoprotein E type 4, ApoE 4, allele is a well known risk factor for the development of late onset Alzheimer disease (LOAD). One avenue to understand the mechanism by which the ApoE 4 allele enhances or advances the progression of the disease is to compare the gene expression in the brain of subjects with genotype E4 versus E3. Previous studies of gene expression in AD have focused on patients of at least 60 years of age suffering LOAD with significant neuropathological burden. One limitation of these studies is that the gene expression associated with inflammation, degenerative, and reactive phenomena can obscure the early pathogenic events of the disease.

Design: In order to test our hypothesis that the various ApoE groups have different gene expressions and that these differences are relevant to the relative group risk for developing Alzheimer disease (AD), we collected frozen frontal lobe tissues from 47 autopsies. The subjects include ApoE 3/3 (n=22) and ApoE 3/4 (n=25) genotypes. All subjects are 30-55 years of age and their brains are free of AD pathology defined as a lack of Aβ deposition and minimal tau deposition (Braak I/II). RNA was extracted from frozen tissue using TRIZOL Reagent (Invitrogen, USA), purified using the RNeasy-kit (RNeasy Lipid Tissue kit; QIAGEN), treated with DNAse (AMBION, DNA-free kit). A minimum RNA integrity number (RIN) of greater to or equal to 7.0 was set as sufficient and reached for each sample utilized. RNA libraries were prepared from 50 μg of total RNA (RIN ≥7) from post-mortem brain tissue. RNA was sequenced on Illumina Next Seq500 platform.

Results: Tissues have been collected and RNA has been extracted. RNAseq library preparation and sequencing have been completed. Analysis of gene expression is in progress.

Conclusion: We will be analyzing the RNAseq data and testing our hypothesis that there is a significant correlation between ApoE groups and their RNA transcriptome. Using this novel approach, we hope to gain insight into up- or down-regulated genes or pathways that may be potential targets for prevention and therapy in an at risk population.

BACKGROUND

- 45% of people over the age of 85 are estimated to have AD and it is the most common neurodegenerative disease in those older than 65.
- Current understanding of disease pathogenesis is that neurodegeneration is due to an imbalance of production and clearance of Aβ peptides in addition to tau.
- Previous studies that assess gene expression are inherently limited due to confounding neurological pathologies in an aging population.

BACKGROUND (CONT)

- Multiple risk factors have been identified in familial and sporadic forms; however, the strongest risk factor for LOAD is ApoE.
- ApoE 4 is associated with increased Aβ deposition, prevalence of AD, and a lower age of onset in a gene dose-dependent manner.
- ApoE 4 is associated with cognitive decline many years before cognitive impairment becomes clinically apparent.
- Furthermore, a study shows there may be Apo E4 benefits during development and early adulthood at the cost of more rapid decline with aging.

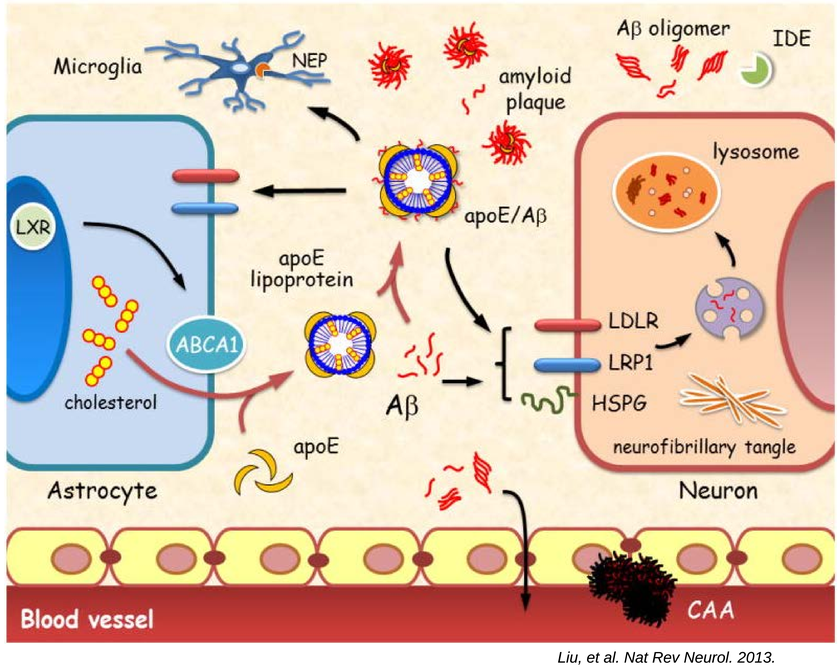

Liu, et al. Nat Rev Neurol. 2013.

DESIGN

- 47 frontal lobe samples were acquired from forensic autopsies under protocols authorized by the IRB of the State of Maryland Department of Health and Human Services.
- Causes of death varied, including motor vehicle accidents, suicide, and non-neurological medical diseases.
- All tissues were free of Aβ on neuropathological examination.

DESIGN (CONT)

- RNA was extracted from frozen tissue using TRIZOL Reagent, purified using the Rneasy-kit, and treated with DNAse.
- A minimum RIN of 7.0 was required for RNA library preparation
- RNA was sequenced on Illumina Next Seq500 platform.

Age	Number of subjects (n=47)	Race	Number of subjects (n=47)
30-40	19	W	36
40-49	24	AA	9
50-55	4	HS	1
		Unk	1
Sex	**Number of subjects (n=47)**	**ApoE**	**Number of subjects (n=47)**
M	30	3/3	22
F	17	3/4	25
Post-Mortem Delay (hrs)	9-44		

CONCLUSIONS & FUTURE DIRECTIONS

Having recently completed our RNAseq library preparation, we will analyze the RNAseq data. In order to test our hypothesis, we will examine if there is a significant correlation between ApoE groups and their RNA transcriptome in a young population without AD pathology. Using this novel approach, we hope to gain insight into up- or down-regulated genes or pathways that may be potential targets for prevention and therapy in an at risk population.

Acknowledgements:
Johns Hopkins University Alzheimer's Disease Research Center (P50AG05146)
BrightFocus Foundation

REFERENCES

- Caselli RJ, et al. Longitudinal modeling of age-related memory decline and the APOE ε4 effect. N Engl J Med. 2009; 361:255–263.
- Corder, E. H., Saunders, A. M., Strittmatter, W. J., et al. 1993. Gene dose of apolipoprotein E type 4 allele and the risk of Alzheimer's disease in late onset families. *Science*. 261:921-923.
- Mondadori CRA, et al. Better memory and neural efficiency in young apolipoprotein E ε4 carriers. Cerebral Cortex. 2007; 17:1934–1947.
- Liu, C.C., Kanekiyo T., Xu H., and Bu G. 2013. Apolipoprotein E and Alzheimer disease: risk, mechanisms, and therapy. *Nat Rev Neurol*. 9(2): 106-118.

Use of Neuroimaging Techniques to Simulate and Evaluate Standard Neuropathology Tissue Sampling

C.S. Latimer[1], T. Madhyastha[2], J.P. Owen[2], C.D. Keene[1], T. Grabowski[2,3]

[1]*Department of Pathology, Neuropathology Division, University of Washington, Seattle, WA,* [2]*Department of Radiology, University of Washington, Seattle, WA and* [3]*Department of Neurology, University of Washington, Seattle, WA*

PROJECT GOALS

- Provide training and background in neuroimaging
- Integrate imaging technology with neuropathology to enhance sampling techniques

✓	Learn to align sampled region in image space to standard template
✓	Investigate sampling consistency in region of interest
	Apply techniques to assess functional anatomical correlates with focus on default mode network
	Develop image-guided approaches to improve routine and targeted sampling
	Apply new techniques prospectively to group of subjects with functional imaging

BACKGROUND

- Current neuropathology sampling protocols are imprecise and neuroimaging data and technology are underutilized
- Relationship of gross landmarks to specific functional cortical fields is variable, especially in association brain regions most vulnerable to AD
- Better characterization of sampling and enhanced targeting may be enabled through ante-mortem and/or post-mortem brain imaging

METHODS

This preliminary analysis simulates neuropathological tissue sampling by virtually sampling 3D MR images and assesses anatomical consistency using standard image processing tools

Subjects: UW ADRC Clinical Core participants (n = 34)

Image Acquisition: High resolution (0.8 mm^2) structural MR images

Virtual Sampling:

- "Sectioned" subject MRIs into 4 mm coronal slices to simulate post-mortem sectioning
- Superior/middle temporal gyrus chosen as representative sampled region
- Rectangular block drawn on image at level of anterior hippocampus to simulate sampling
- Mask generated from sampled area to separate out region of interest in imaging software
- Individual masks warped to standard space through registration process and averaged to demonstrate total area covered and degree of overlap

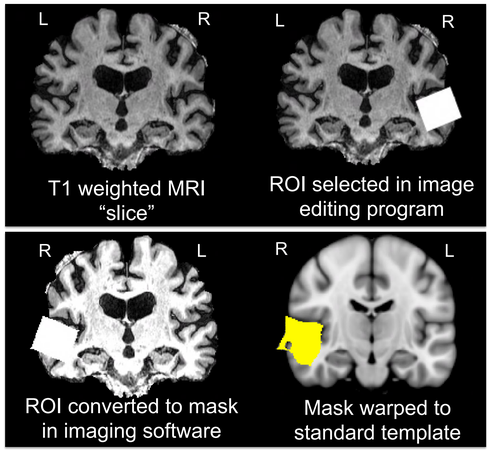

Image Registration: Process of conforming individual MR images to standard template

- Distorts individual images but allows for comparison between subjects and to standard

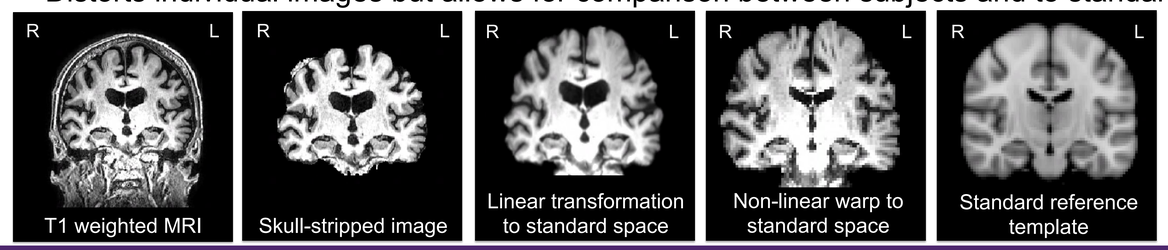

Quality Control: Visual Inspection

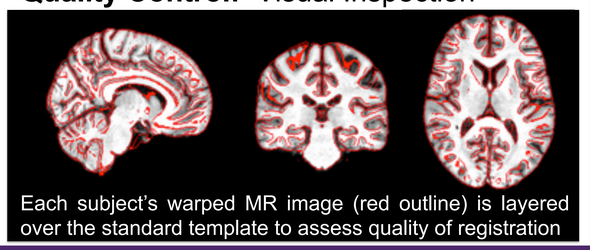

PRELIMINARY RESULTS

There is individual variation in sampling with relatively little overlap

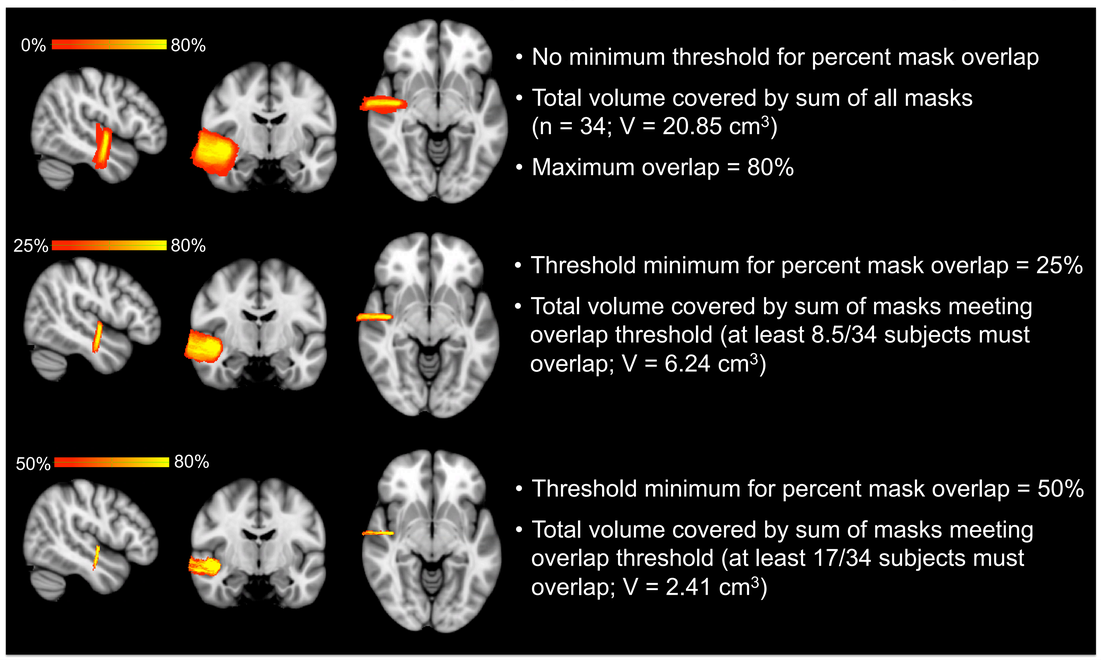

- No minimum threshold for percent mask overlap
- Total volume covered by sum of all masks (n = 34; V = 20.85 cm^3)
- Maximum overlap = 80%
- Threshold minimum for percent mask overlap = 25%
- Total volume covered by sum of masks meeting overlap threshold (at least 8.5/34 subjects must overlap; V = 6.24 cm^3)
- Threshold minimum for percent mask overlap = 50%
- Total volume covered by sum of masks meeting overlap threshold (at least 17/34 subjects must overlap; V = 2.41 cm^3)

Mask volume rapidly declines with increasing threshold minimum

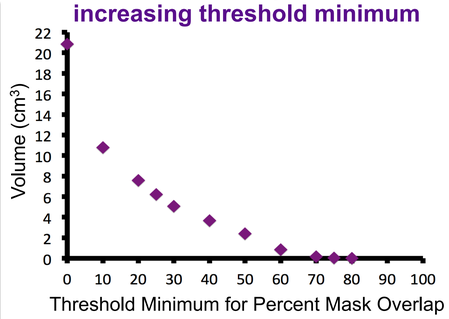

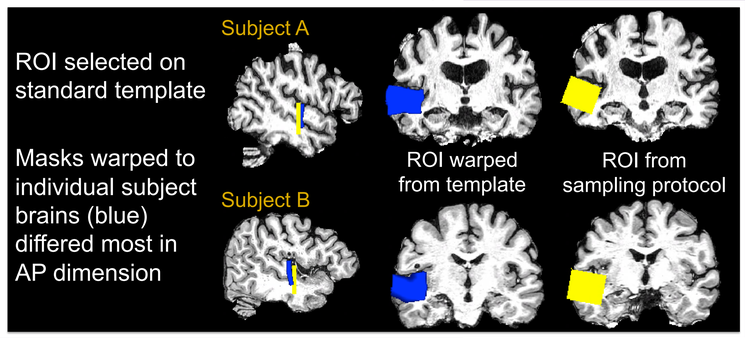

FUTURE DIRECTIONS

1. Additional quality control
   - Double check coding
   - Run additional registrations protocols
2. Evaluate factors contributing to poor overlap
   - Pathologist dependent
   - Sectioning dependent
   - Anatomic landmarks
3. Focus on default mode network
   - Evaluate functional anatomical correlates of current cortical sampling scheme
4. Develop and test new image-guided techniques to improve sampling
   - Target default mode network
   - Sample radiographically defined lesions not seen grossly

REFERENCES

Raichle, M. E. The brain's default mode network. *Annual review of neuroscience* 38, 433-447 (2015)

Amunts, K. & Zilles, K. Advances in cytoarchitectonic mapping of the human cerebral cortex. *Neuroimaging clinics of North America* 11, 151-169, vii (2001).

Avants B. B. *et al.* The Insight ToolKit image registration framework. *Frontiers in Neuroinformatics* 8, 44 (2014)

ACKNOWLEDGEMENTS

Supported by the National Institutes of Health grant P50 AG005136

UCSF Weill Institute for Neurosciences
Memory and Aging Center

Astrocytic tau deposition is frequent in Alzheimer disease and does not correlate with an atypical clinical presentation

Amber Nolan, Elisa De Paula Franca Resende, Cathrine Petersen, Kyra Neylan, Salvatore Spina, Bruce Miller, William Seeley, Lea T. Grinberg

Background

Classical Alzheimer disease (AD) features an evolving amnestic syndrome that reflects progression of pathology through specific neural networks. However, a subset of patients exhibit atypical onset with prominent language, behavioral, or visuospatial deficits. Despite this variability, CERAD, Thal and Braak staging schemes still correlate with disease progression and do not explain the clinical heterogeneity observed. Tau astrogliopathy is common in the aging brain, but has yet to be systematically characterized outside the temporal lobe and in relation to AD pathology. Evidence suggests that clusters of tau-positive thorny astrocytes in the inferior frontal gyrus associate with a primary progressive aphasia phenotype in an AD cohort (1). Thus, we hypothesize that co-existing tau astrogliopathy may change vulnerability of cortical networks to AD pathology and explain clinical heterogeneity. To investigate this hypothesis, we systematically mapped the presence and density of tau in astrocytes throughout selected cortical and subcortical sections in a cohort of patients enriched for atypical presentations of Alzheimer disease to correlate with clinical characteristics.

Methods

Cases
- 76 patients with a neuropathologic diagnosis of Alzheimer disease of variable severity, with or without argyrophilic grain disease, excluding cases with FTLD (FUS, tau, TDP-43) and alpha-synuclein pathologies.

Pathology Analysis
- Assessed for tau pathology in astrocytes using 8 micron-thick sections immunostained for phosphorylated tau (CP-13, 1:500, gift from Dr. Peter Davies)
- Astrocytic tau was classified according to the recent harmonized evaluation strategy (2):
  - Thorn-shaped astrocytes(TSA) which can be identified in white matter, grey matter, perivascular, subpial, or subependymal locations.
  - Granular or fuzzy astrocytes (GFA) which are found in grey matter.
- The presence or absence of these morphologies in these locations, as well as the highest density in a 20X microscopic field, was quantified in each area listed below.
- Of note, we use the term aging-related tau astrogliopathy (ARTAG) to indicate the presence of tau in an astrocyte with either a TSA or GFA morphology in any location. We use the term argyrophilic thorny astrocyte clusters (ATAC) to specifically indicate the presence of thorn-shaped astrocytes (TSAs) in the white matter, usually occurring in clusters at the grey-white junction.
- The hippocampus, inferior frontal cortex, and the amygdala were also evaluated for argyrophilic grain disease (AGD). The presence of AGD was determined by having 3 of 4 criteria in the hippocampus (1- grains, 2- coiled bodies, 3- eyeliner sign in CA2, 4- tau inclusions in the dentate) and the presence of grains and coiled bodies in the amygdala or inferior temporal cortex (3).
- The areas examined included the following: anterior cingulate cortex, middle frontal gyrus, inferior frontal gyrus, inferior temporal gyrus, amygdala, insular cortex, putamen, entorhinal/perirhinal cortex, and the angular gyrus.

Clinical Data
- Prior to autopsy, patients were recruited from the Memory and Aging Center at the University of California, San Francisco. They were evaluated through in depth neurological history, examination and extensive neuropsychological assessment. Clinical diagnosis was determined by consensus from a team of clinicians based on published criteria.
- Main cognitive domains were assessed through a pre-defined calculated composite score using z scores from the collected neuropsychological raw data (4).
  - An executive function score was calculated using speed processing and set shifting from the trail making test, word generation from lexical fluency, control inhibition from Stroop test and attention from the digit backwards test.
- A history of traumatic brain injury (TBI) was determined from the Uniform Dataset Questionnaire, autopsy report and chart review. A definite positive history of TBI included a hit to the head with or without loss of consciousness for any amount time. A possible history of TBI included cases without explicit history but risk factors of sports contact, falls, domestic violence, military blast or car accident. TBI was considered absent after in depth review of the chart with no documented history of a hit to the head and no risk factors.

Statistics
- Statistical analyses were performed using R Statistical Software (version 3.3.3; R Foundation for Statistical Computing, Vienna, Austria).
- A Chi Square test was used to analyze the relationships between the different pathologies and the incidence of co-pathology. The graphic is a visualization of the correlation coefficients between each pair of pathologies.
- Principal component analysis was used to analyze the relationships between ARTAG presence in different brain regions with a varimax rotation with four factors.
- Univariate and multivariate logistic regression was used to evaluate the relationship between overall pathology presence and clinical characteristics, accounting for age of death, sex, history of TBI, atypical diagnosis, and presence of AGD.
- Multiple t-tests were used to analyze ATAC density in different areas as a function of TBI.
- A Chi Square test was used to analyze the differences in pathology presence in each frontal brain region between cases diagnosed as FTD and others. A Mann-Whitney test was used to analyze the differences in pathology densities in each frontal brain region between cases diagnosed as FTD and others.
- P-values ≤0.05 were considered statistically significant.

Overview of Demographics and Frequency of Pathologies

Demographics by Diagnosis

Clinical Diagnosis	Number	Proportion Male	Mean Age of Death (YRS)	Mean Disease Duration (YRS)	Mean Education (YRS)	Proportion with ARTAG
AD	44	0.73	73.23	10.14	15.83	0.70
FTD	6	0.83	67.00	13.83	16.25	0.67
CBS	6	0.17	68.83	9.17	16.67	0.50
PCA	5	0.20	62.40	9.00	15.80	0.40
PPA	4	0.50	68.75	9.25	16.25	0.50
CJD	1	1.00	66.00	8.00	16.00	1.00
MCI	7	0.43	82.00	8.43	16.14	0.71
Control	3	1.00	85.33	NA	15.00	1.00
TOTAL	76	0.63	72.63	10.04	15.94	.67

Pathology by Diagnosis

Clinical Diagnosis	Proportion with ATAC	Proportion with GMA			Proportion with Subpial	Proportion with Subependymal	Proportion with Perivascular
		All Types	TSA	GFA			
AD	0.59	0.50	0.23	0.18	0.34	0.30	0.23
FTD	0.33	0.33	0.33	0.17	0.50	0.50	0.50
CBS	0.50	0.17	0.17	0.00	0.17	0.17	0.00
PCA	0.40	0.00	0.00	0.00	0.00	0.00	0.00
PPA	0.50	0.25	0.25	0.00	0.00	0.25	0.00
CJD	0.00	0.00	0.00	0.00	0.00	1.00	0.00
MCI	0.29	0.43	0.29	0.29	0.57	0.14	0.14
Control	0.33	0.67	0.00	0.67	0.67	1.00	0.67
TOTAL	0.50	0.29	0.21	0.17	0.33	0.30	0.21

Patterns of Astrocytic Tau Deposition

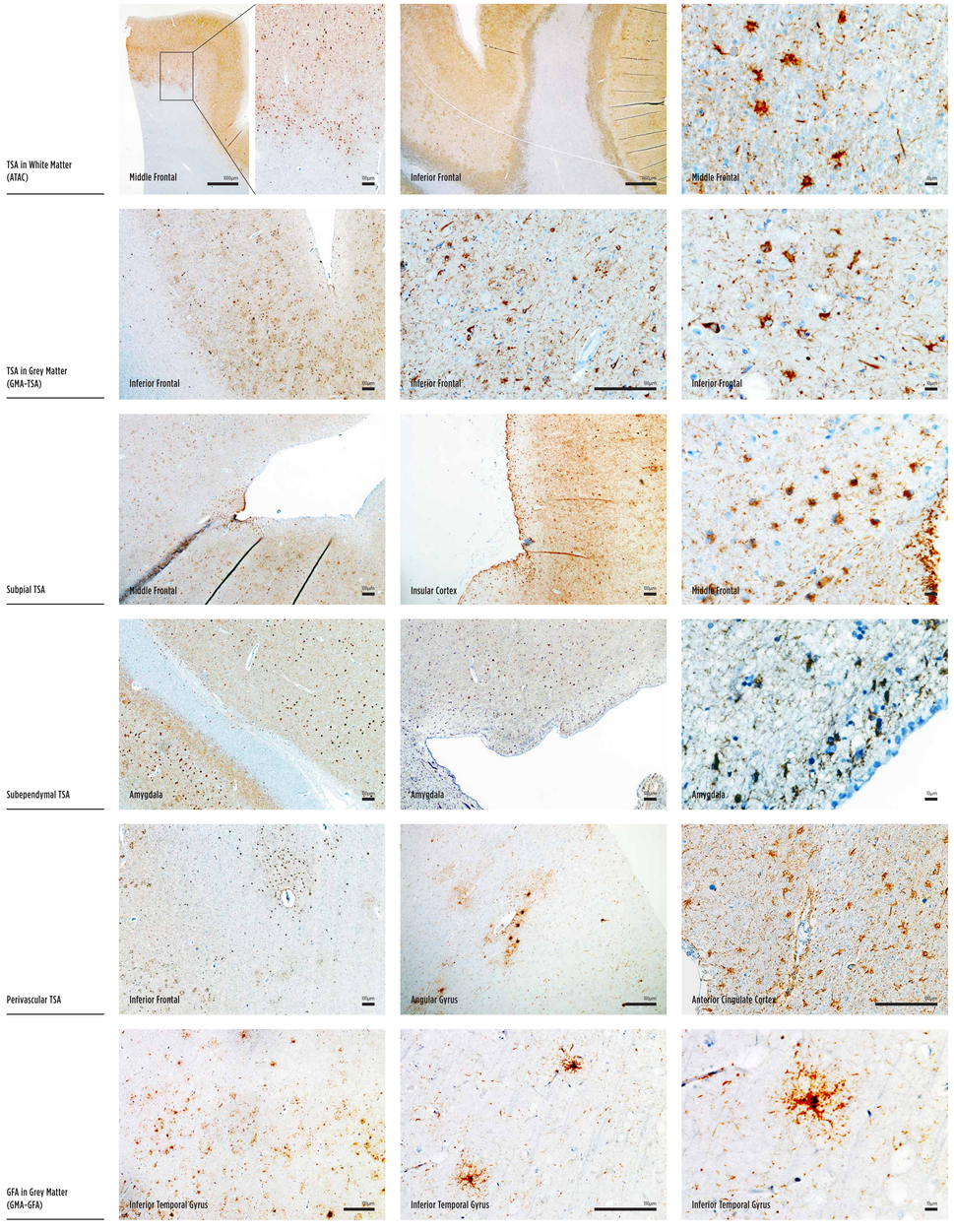

Abbreviations: AD- Alzheimer disease, classic clinical phenotype, FTD- frontotemporal dementia clinical phenotype, CBS- corticobasal syndrome, PCA- posterior cortical atrophy clinical syndrome, CJD- Creutzfeldt-Jakob Disease, MCI- mild cognitive impairment, TSA- thorn-shaped astrocytes, ATAC- thorn-shaped astrocytes in the white matter, GMA- astrocytes with tau accumulation in the grey matter, either thorn-shaped or granular/fuzzy morphology, GMA-TSA- thorn-shaped astrocytes in the grey matter, GFA- granular or fuzzy astrocytes, GMA-GFA- granular/fuzzy astrocytes in the grey matter, SP- subpial TSAs, PV- perivascular TSAs, aCC- anterior cingulate, MFG- middle frontal gyrus, IFG- inferior frontal gyrus, ITG- inferior temporal gyrus, InsC- insular cortex, Put- putamen, EC- entorhinal/perirhinal cortex, Amgy- amygdala, AG- angular gyrus.

The presence of co-pathology within subtypes of astrocytic tau is frequent and significant

Frequencies of Additional Pathology Subtypes, p value <0.001 for all relationships

	Frequency ATAC (%)	Frequency GMA (%)	Frequency GMA-TSA (%)	Frequency GMA-GFA (%)	Frequency Subpial (%)	Frequency Perivascular (%)
ATAC	–	35.71	24.60	15.87	31.74	34.12
GMA	64.28	–	57.14	54.28	42.85	31.42
GMA-TSA	77.50	–	–	20.00	47.50	42.50
GMA-GFA	52.63	–	21.10	–	36.84	26.31
Subpial	62.50	46.80	29.70	21.90	–	34.30
Perivascular	75.40	38.60	29.80	17.50	38.60	–

Correlation of Relationships between Pathology Subtypes

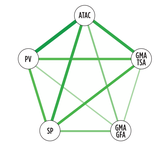

The distribution of astrocytic tau pathology is clustered into distinct anatomical regions

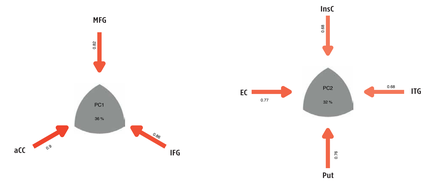

Logistic regression analysis did not find a relationship between an atypical clinical diagnosis and astrocytic tau pathology

Relationship of Presence of ARTAG Pathology to Clinical Diagnosis and Demographics

Variables	Univariate Logistic Regression (n= 76)		Multiple Logistic Regression (Age, Sex, Atypical dx, AGD) n=76		Multiple Logistic Regression (Age, Sex, TBI, Atypical dx, AGD) n=40	
	Coefficient Estimate (std error)	p Value	Coefficient Estimate (std error)	p Value	Coefficient Estimate (std error)	p Value
AGE	0.082 (0.028)	**0.0388**	0.074 (0.031)	**0.0169**	0.145 (0.061)	**0.0189**
SEX	1.23 (5.3e-1)	**0.0175**	1.087 (0.559)	0.0518	1.156 (0.944)	0.2208
TBI	1.45 (0.865)	0.0973	–	–	1.599 (1.091)	0.1425
Atypical Clinical Diagnosis	-0.775 (0.525)	0.1408	-0.039 (0.600)	0.9482	0.448 (0.996)	0.6528
Presence of AGD	1.340 (1.099)	0.2227	0.331 (1.181)	0.7795	-2.123 (1.583)	0.1799

Relationship of Subtypes of Tau Astropathology to Clinical Diagnosis and Demographics

Multiple Logistic Regression Analysis (Age, Sex, TBI, Atypical dx, AGD) n=40

Variables	ATAC		GMA-GFA		Subpial		Subependymal		Perivascular	
	Coefficient Estimate (std error)	p Value	Coefficient Estimate (std error)	p Value	Coefficient Estimate (std error)	p Value	Coefficient Estimate (std error)	p Value	Coefficient Estimate (std error)	p Value
AGE	0.069 (0.042)	0.0988	0.186 (0.077)	0.1172	0.197 (0.076)	**0.0019**	0.166 (0.072)	**0.0213**	0.260 (0.129)	**0.0434**
SEX	-1.175 (0.845)	0.1642	2.329 (1.1809)	0.1979	1.663 (1.147)	0.2022	2.266 (1.137)	**0.0462**	2.349 (1.730)	0.1765
TBI	1.683 (0.852)	**0.0483**	0.768 (1.239)	0.5355	2.274 (1.181)	0.0542	0.655 (0.892)	0.4650	2.408 (1.423)	0.0905
Atypical Clinical Diagnosis	-0.665 (0.905)	0.4637	1.092 (2.999)	0.6954	0.137 (1.447)	0.9247	1.857 (1.375)	0.1814	3.948 (2.415)	0.1021
Presence of AGD	-2.518 (1.406)	0.0735	3.065 (1.527)	**0.0448**	0.477 (1.447)	0.7416	1.252 (1.370)	0.3606	0.765 (1.481)	0.6055

An increased density of ATACs in the anterior cingulate cortex is associated with a history of TBI

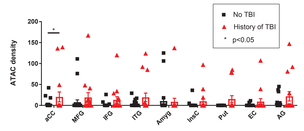

In depth analysis of FTD and astrocytic tau in frontal and insular cortices does not reveal a significant relationship

Frequency of ARTAG Pathology by FTD diagnosis in Frontal and Insular Cortices

Dx of FTD (n)	Anterior Cingulate (%)	Middle Frontal (%)	Inferior Frontal (%)	Insula (%)	Any Frontal/Insular Area (%)
No (70)	26	27	26	23	41
Yes (6)	0	17	17	5	33
p value	0.1272	0.576	0.6253	0.1406	0.6986

Frequency of ATAC Pathology by FTD diagnosis in Frontal and Insular Cortices

Dx of FTD (n)	Anterior Cingulate (%)	Middle Frontal (%)	Inferior Frontal (%)	Insula (%)	Any Frontal/Insular Area (%)
No (70)	23	21	21	16	37
Yes (6)	0	17	17	0	17
p value	0.1875	0.7836	0.7836	0.2937	0.3145

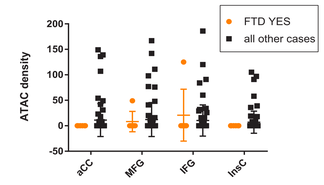

There is no correlation with executive function and astrocytic tau in frontal and insular cortices

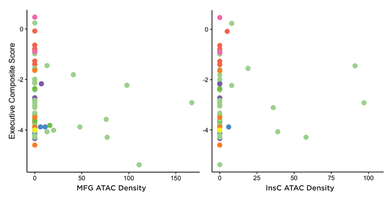

Conclusions

No obvious relationship between atypical AD and tau accumulation in astrocytes is identified in this study.

However, there is a trend for an increase in thorn-shaped astrocytes in the white matter with a history of traumatic brain injury; in particular, the anterior cingulate cortex appears to demonstrate a significantly higher density of ATACs with TBI compared to no history of head injury.

We identified a correlation with the presence of granular/fuzzy astrocytes and argyrophilic grain disease.

There is an overall increase in astrocytic tau with increasing age, similar to previous reports.

The subtypes of astrocytic tau are commonly identified together and seem to cluster by anatomical region.

References

1. Munoz DG, Woulfe J, Kertesz A. Argyrophilic thorny astrocyte clusters in association with Alzheimer's disease pathology in possible primary progressive aphasia. Acta Neuropathol. 2007;114:347–357.
2. Kovacs GG, Ferrer I, Grinberg LT, et al. Aging-related tau astrogliopathy (ARTAG): harmonized evaluation strategy. Acta neuropathological 2016;131(1):87-102.
3. Rodriguez RD, Suemoto CK, Molina M, et al. Argyrophilic Grain Disease: Demographics, Clinical, and Neuropathological Features From a Large Autopsy Study. J Neuropathol Exp Neurol. 2016 Jul;75(7):628-35.
4. Knopman DS, Kramer JH, Boeve BF, et al. Development of methodology for conducting clinical trials in frontotemporal lobar degeneration. Brain. 2008;131(11):2957-2968.

Acknowledgements

Research reported in this publication is supported by NIH Grant K24AG053435, NIH Grant P01AG019724, and the National Institute On Aging of the National Institutes of Health under Award Number P50AG023501. In addition, Elisa de Paula Franca Resende is an Atlantic Fellow at the Global Brain Health Institute (GBHI) and thanks GBHI for supporting her work. Amber Nolan thanks the UCSF Department of Pathology for their support.

Patient-derived induced pluripotent stem cells from brain donors for the study of Alzheimer's disease and other neurodegenerative disorders.

Massachusetts Alzheimer Disease Research Center[1], C S Kubik Laboratory for Neuropathology[2] & Neurology Service[3]
Massachusetts General Hospital, Harvard Medical School, 114 16th Street, Charlestown, MA 02129
Derek H. Oakley, M.D., Ph.D.[1,2], Naomi Klickstein[1], Bradley T. Hyman M.D., Ph.D.[1,3], & Matthew P. Frosch, M.D., Ph.D.[1,2]

Introduction:

Patient-derived induced pluripotent stem cell (iPS cell) models of neurodegenerative disease are of growing importance in our attempts to understand these disorders. An ongoing challenge in this work is that selection of cases and controls for iPS line derivation is often based on clinical criteria and lacks the definitive confirmation provided by neuropathologic evaluation at autopsy. Furthermore, there are still unanswered questions regarding how well iPS-derived neurons reflect cells within individual matched donor brains and whether features of clinical and pathologic variation are recapitulated in patient-derived neurons that have not undergone a lifetime of exposure to the cellular milieu of the brain.

To address these issues, we are building a resource of iPS lines and matched brain tissues derived from patients who have undergone clinical evaluation before ultimately coming to autopsy. To date, we have derived primary fibroblasts from over 70 brain donors with neuropathologic diagnoses including Alzheimer's disease (AD), familial AD (FAD), familial cerebral amyloid angiopathy (CAA), frontotemporal dementia (FTLD), Lewy body disease (LBD), multiple system atrophy (MSA), progressive supranuclear palsy (PSP), amyotrophic lateral sclerosis (ALS), Wolfram syndrome, and controls without significant neuropathologic findings. Many of these lines have been reprogrammed to iPS cells using a non-integrating mRNA approach. Once characterized, iPSC lines will be deposited in a cell bank and made available to other researchers.

Consent for autopsy and iPSC generation:

To provide informed consent for this project, we developed an IRB-approved autopsy permit rider that includes consent for iPSC generation and use in research (including genetic studies), teaching, and distribution to other researchers in a manner that is consistent with MGH policies.

Fibroblast derivation:

- At the time of brain donation, a 1-2 square cm piece of skin is sterilely removed from the thigh.
  - Care is given to take as little subcutaneous fat as possible.
- Skin samples are transported in sterile saline and held at 4C until dissection
- Tissue is microdissected into 1-2 mm fragments (Figure 1A)
- Attachment to treated T75 flasks at RT for ~5 minutes (Corning Cellbind)
- Fed with fibroblast media, low volume (5-7 mL)
- Media changed once per week
- 80-90% confluence in ~4 weeks (Figure 1B-C)
- Tissue fragments removed
- Fibroblasts trypsinized and cryopreserved using isopropanol freezing chambers

Fibroblast culture medium: DMEM, 10% FBS, L-glutamine, Antibiotic-Antimycotic.
Freezing medium: Synth-a-Freeze.

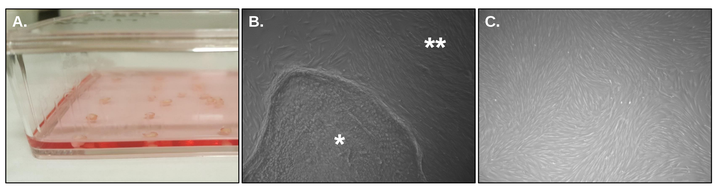

Figure 1: Explant derivation of primary human fibroblasts.
(A) 1-2 square mm tissue fragments evenly distributed throughout T75 flask. (B) Initially, keratinocytes (*) dominate explant growth and are subsequently overgrown by fibroblasts (**). (C) cultures become confluent over the course of 4-6 weeks.

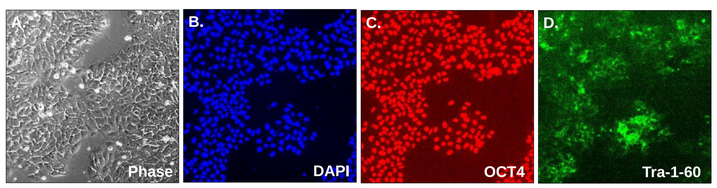

Figure 2: Reprogramming fibroblasts to iPSCs.
Reprogramming of primary fibroblast lines was carried out using a non-integrating mRNA approach to avoid undesired disruption of endogenous genes (Cellular Reprogramming Inc). The selected iPSC line is from a familial Alzheimer's disease patient harboring a PSEN1 mutation (see below). (A) Reprogrammed iPSCs grown on rLamanin-521 substrate display a typical morphology under phase contrast and (C) DAPI. The iPSCs express pluripotency markers (C) OCT-4 and (D) Tra-1-60 by immunohistochemistry (IHC).

Table 1: Current fibroblast and iPSC lines.

Final Pathologic Diagnosis:	Fibroblast Lines	Reprogrammed iPSC Lines	Median Age	Age Range	Average Thal	Average Braak	Average CERAD (1-3)
Alzheimer's Disease (AD)	17	7	85	57 - 90+	4.5	5.6	2.5
Familial AD (PSEN1 L435F and A163G)	2	1	--	53 - 59	5	6	3
Control	3	2	>90	79 - 90+	0	1.3	0
Familial Cerebral Amyloid Angiopathy (APP L34V)	1	0	63	--	0	0	0
AD + Lewy Body Disease (at least Braak 4 of 6)	4	2	81	59 - 90+	4.5	5.5	2.5
Lewy Body Disease (at least Braak 4 of 6)	5	2	79	61 - 90+	2.8	2.4	1.4
Frontotemporal Lobar Degeneration (FTLD)	7	4	69	55 - 73	--	--	--
Progressive Supranuclear Palsy (PSP)	4	2	69	61 - 73	0.5	0.3	0.25
Multiple System Atrophy (MSA)	4	2	67	52 - 70	0.75	--	--
Amyotrophic Lateral Sclerosis (ALS)	2	1	--	48 - 61	--	--	--
Wolfram Syndrome	1	1	69	--	--	--	--
White matter gliosis (AD clinical phenotype)	1	1	78	--	--	1	--
Atypical cerebellar degeneration	1	1	63	--	--	--	--
Bilateral SDH (PSP clinical phenotype)	1	0	65	--	--	--	--
AD pending final pathology	6	0					
Controls pending final pathology	3	0					
Huntington's disease pending final pathology	1	0					
Others pending final pathology	11	0					
Totals:	**74**	**26**					

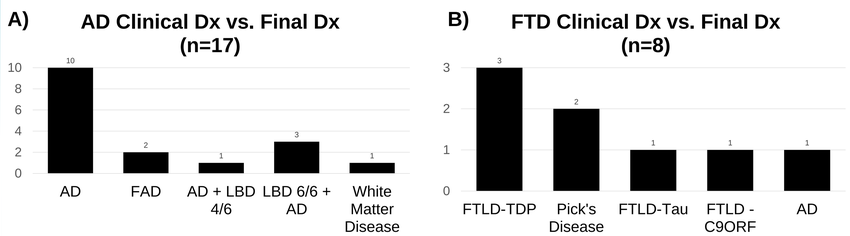

Figure 3: Clinicopathologic correlation.
Mismatches between clinical and pathologic diagnoses highlight the importance of autopsy in assembling banks of iPSCs focused on neurodegenerative disease. (A) Four cases with a clinical diagnosis of AD had overlapping LBD pathology and one demonstrated extensive white matter disease in the absence of AD neuropathologic changes (n=17). (B) Of 8 FTD cases collected, pathologic diagnoses were variable, as expected for this clinical entity. (C) Of 5 Control cases collected, one showed extensive AD neuropathologic changes and one showed moderate LBD with mild AD neuropathologic changes. (D) Within the pure ADNC final diagnosis group (19 cases), there were 7 cases that did not exhibit a standard AD clinical phenotype. *=additional thalamic degeneration.

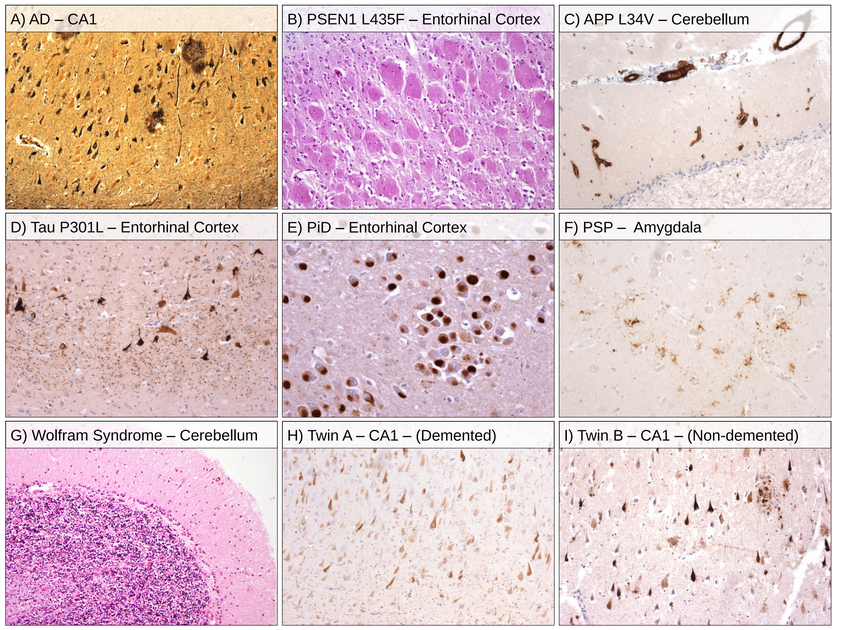

Figure 4: Select cases of interest.
Examples of fibroblast donor cases: (A) Alzheimer's disease, Bielschowsky silver stain. (B) Familial Alzheimer's disease (PSEN1 L435F), Luxol H&E. (C) Familial CAA (APP L34V, Piedmont mutation), beta-amyloid IHC. (D) FTLD-Tau (P301L), Tau IHC. (E) Pick's Disease, Tau IHC. (F) Progressive supranuclear palsy (PSP), Tau IHC. (G) Wolfram syndrome, Luxol H&E. (H & I) depict identical twins discordant for dementia, both with AD pathology, Tau IHC (NIA-Reagan Intermediate and A3B3C2 respectively). Twin B was a fibroblast donor.

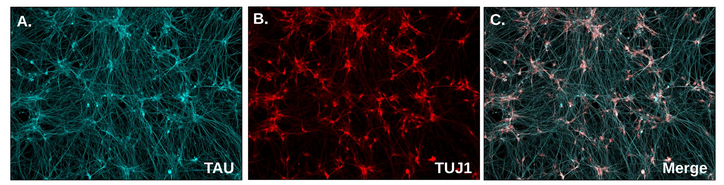

Figure 5: Cortical neurons from iPSCs (Non-MADRC generated iPS line).
We currently produce iPS-derived cultures of layer II/III cortical neurons using inducible expression of Neurogenin 2 (Ngn2) (1). This process yields high-purity cultures of postmitotic neurons that express (A) Tau and (B) TUJ1 by immunohistochemistry. (C) Merged.

Future directions:

- Genotyping of iPSCs and matched donor brains
- Deposit for eventual distribution
- Direct conversion of MADRC iPSCs into neurons via inducible Ngn2
- Multi-omic comparison of iPS-neurons to matched donor brain neurons
- Assessment of established pathologic correlates of AD and FTLD in iPS-neurons

Acknowledgements:

D.H.O. is supported by an administrative supplement through the Massachusetts Alzheimer Disease Research Center (MADRC) (P50 AG05134). Collection of fibroblasts and subsequent reprogramming is covered under an amendment to the ADRC Neuropathology Core IRB protocol (1999p009556). iPS cell generation is a collaboration with the Novartis Institutes for Biomedical Research, Cambridge MA.

References:
1. Zhang Y, Pak C, Han Y, Ahlenius H, Zhang Z, Chanda S, Marro S, Patzke C, Acuna C, Covy J, Xu W, Yang N, Danko T, Chen L, Wernig M, Südhof TC. Rapid single-step induction of functional neurons from human pluripotent stem cells. Neuron. 2013 Jun 5;78(5):785-98.

Center for Neurodegenerative Disease Research
University of Pennsylvania

Comprehensive analysis of myeloid cells across neuropathological stages of Alzheimer's disease (AD) and related dementias (RD)

Perelman School of Medicine
University of Pennsylvania

Stefan Prokop[1], Kelly R. Miller[1,2], Sergio Rodriguez Labra[1], Rose M. Pitkin[1], John Robinson[1], Edward B. Lee[1], Virginia M.-Y. Lee[1], John Q. Trojanowski[1]

Author Affiliations:

[1] AD Center Core (ADCC), Center for Neurodegenerative Disease Research, Department of Pathology and Laboratory Medicine, University of Pennsylvania (PENN) School of Medicine, Philadelphia, PA 19104, USA.

[2] present address: Nanostring Technologies, Seattle, WA 98109, USA.

Introduction

The pathognomonic protein deposits in ADRD elicit an activation of myeloid cells, namely microglia with some presumed contribution by peripheral myeloid cells. The role of this immune activation in the course of ADRD is controversial, because mouse models of ADRD pathology do not fully capture the complex human disease condition. A comprehensive analysis of myeloid cells in different stages in human AD brains will lay the groundwork for mapping the myeloid cell response towards extracellular and intracellular pathologies over a broad spectrum of RD, and is in line with a major theme of the PENN ADCC's comparative studies of ADRD.

Aims

- Morphologic characterization of myeloid cells in different stages of AD and ADRD
- Correlation of changes in myeloid cell morphology with pathological changes in different stages of AD and ADRD as well as clinical and biomarker data
- Augmentation of morphologic findings with immunohistochemical, biochemical and molecular analysis of pathologic proteins and markers of microglial activation

Microglia scoring in AD and ADRD

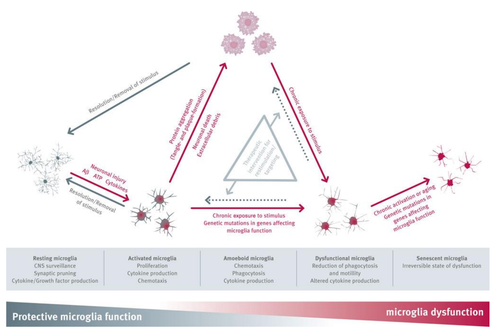

Prokop, S, Miller K & Heppner, F, *Acta Neuropathol* 2013

40µm thick paraffin sections stained with pan-microglia marker Iba1

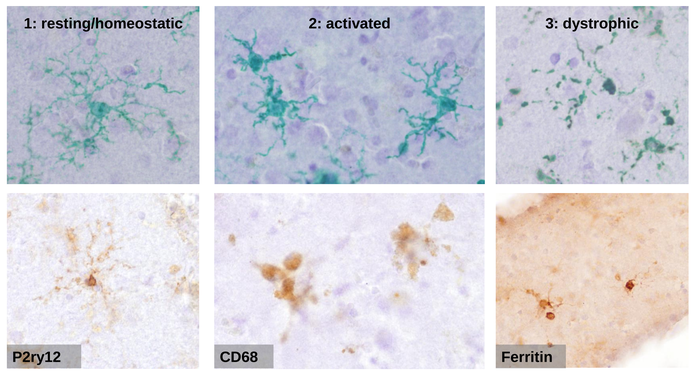

Markers specific for microglia activation states 40x objective

Study cohorts and brain regions for analysis

	No AD	Low	Intermed.	High	High (Trem2 R47H)
N	15	14	6	17	15
Mean age	64.4	70.71	83.67	78.94	76.8
Gender (M/F)	9/6	8/6	3/3	8/9	7/8
Mean PMI	16.1	16	14.33	15.66	13.93

Pathological groups defined according to current neuropathological guidelines (Hyman et al., *Alzheimers Dement.* 2012 Jan;8(1):1-13. doi: 10.1016/j.jalz.2011.10.007.)

Brain regions for analysis:

- Hippocampus
- Frontal cortex
- Visual cortex (striate and peristriate area)
- Cerebellum

Preliminary data on microglia analysis in AD

Scoring of microglia morphology

Scoring of microglia morphology in two select brain regions

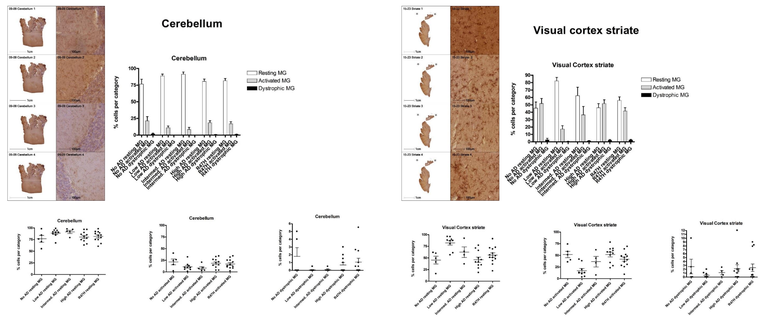

Independent and blinded scoring of microglia morphology in representative images of respective brain regions – between 150 to 400 individual cells scored per region

Correlation of morphologic scoring between two raters

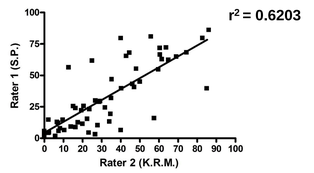

Microglial abundance in analyzed brain regions

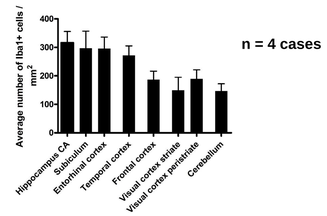

Spatial relation of microglia and protein pathology

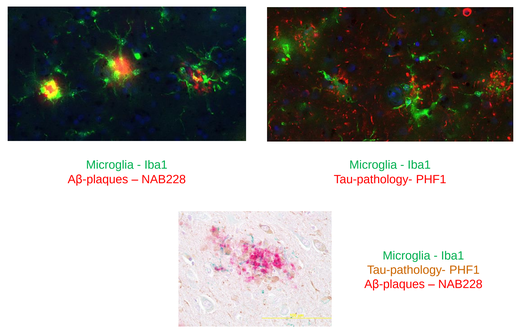

Microglia - Iba1
Aβ-plaques – NAB228

Microglia - Iba1
Tau-pathology- PHF1

Microglia - Iba1
Tau-pathology- PHF1
Aβ-plaques – NAB228

Spatial correlation of microglia and protein pathology in high AD cases (top row – double Immunofluorescence labeling of 40µm paraffin sections; bottom row – triple immunocytochemical labeling of 6 µm paraffin sections)

Detailed analysis of pathology burden

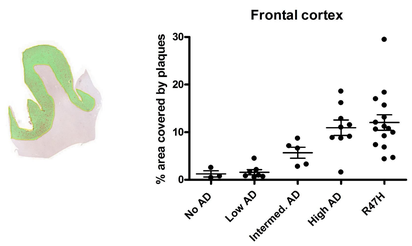

Detailed analysis of Aβ-pathology (NAB228 staining) in frontal cortex sections using Halo® (indica labs) software

Summary and Outlook

- Preliminary data indicate an increase in morphologically activated microglia with progression of AD pathology and demonstrate regional differences in microglial abundance
- Completion of microglia morphology scoring
- Validation of morphological findings with immunohistochemical, biochemical and molecular studies
- Correlation of microglia activation states with Aβ- and Tau pathology (triple labeling and software-assisted detailed image analysis)
- Correlation of morphologic findings with available clinical, genetic and biomarker data

Funding: Supplement to NIH/NIA P30 AG010124

Blood and Brain-Derived Neuronal Exosome Cargo in the Propagation and Progression of Neuropathology

Charisse N. Winston[1], Jonny C. Akers[3], Bob S. Carter[4], Eliezer Masliah[1,2], Robert A. Rissman[1]

[1]Shiley-Marcos Alzheimer's Disease Research Center, [3]Department of Pathology, [3]Cancer Center, and [4]Department of Neurosurgery, UC San Diego

Background

- Tau is a tubulin-binding protein that stabilizes the neuronal cytoskeleton and plays a crucial role in neuronal polarity, structure and axonal transport[1]. In Alzheimer's disease (AD), tau protein becomes hyperphosphorylated (p-tau) and aggregates as neurofibrillary tangle pathology (NFT)[2].
- In humans there are 6 isoforms of tau and in patients with AD, the triple repeat (3R) and quadruple (4R) repeat tau accumulate[3].
- Under pathological conditions, studies have shown that tau aggregates are secreted and can propagate from neuron to neuron in a prion-like manner[4]. The precise mechanisms of tau release in AD are not completely understood, however recent studies suggest that tau may be transported via exosomes[5] and released into the CSF and blood[6].
- The trafficking of tau in exosomes from the CNS to CSF and blood may be an important pathway for identifying stages of AD and identify patients in preclinical stages when pathology is developing and no overt cognitive effects are seen.
- Here, we test the hypothesis that potentially pathogenic forms of tau are released in exosomal vesicles that are positive for the L1 cell adhesion protein (LI CAM). These L1 neuronally-derived exosomes (LINE's) will seed tau aggregation and induce NFT pathology in mice.

Methods

Aim 1: Characterization of tau-contianing LINE's from prodromal and advanced AD cases

Isolation of LINE's from the blood of AD patients and controls

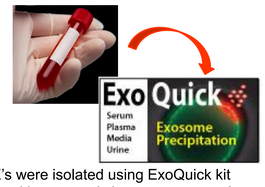

LINE's were isolated using ExoQuick kit followed by magnetic immunocapture of exosomes against L1-CAM antibody

1 Characterization of LINE's by size and TEM

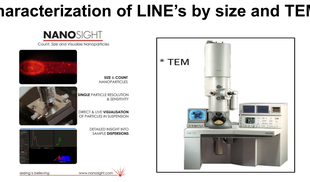

2 Biochemical analysis of LINE's

- Western blot to identify tau and Aβ species contained in LINE's
- Immunogold labeling against PHF-1 antibody to identify p-tau species in exosomes derived from control and AD brains

3 Injection of LINE's into wild-type mice

- LINE preparations from control and AD brains were injected into the hippocampus of wild-type mice and analyzed by immocytochemistry 2m post injection

Aim 2: Characterization of LINE-containing tau species in tau transgenic (Tg) mice

- Western blot to identify tau species in hippocampal samples derived from 3R and 4R Tau Tg mice lines
- qRT-PCR to measure mRNA expression
- Immunogloldlabeling against PHF-1 antibody to identify neurofibrillary tau (NFT) pathology in 3R and 4R Tau Tg mice

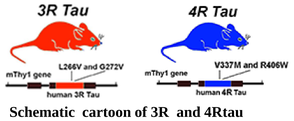

Schematic cartoon of 3R and 4Rtau mouse under the mTHy1 promoter.

Results

Characterization of L1 exosomes based on size and TEM

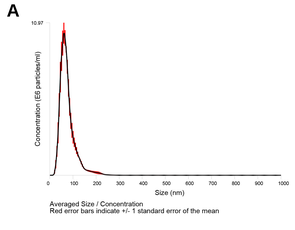

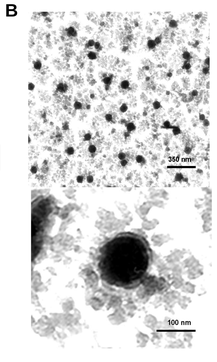

Representative plot of nanoparticale tracking analysis which detected a high concentration of L1 positive exosomes from well-characterized patients with mild cognitive impairment (MCI) compared to controls **A)** (n = 4/group, samples descriptions, see *Grundman et al., 2004*) Representative transmission electron microscopy (TEM) image of L1 positive exosomes isolated from human plasma samples derived from autopsy confirmed AD cases. Samples acquired through the UCSD ADCS Biomarker Core and from the UCSD ADRC bank **B)**. (scale bar 350 nm; 100 nm).

LINE's containing p-tau and $A\beta_{42}$ were significantly increased in human plasma from AD patients

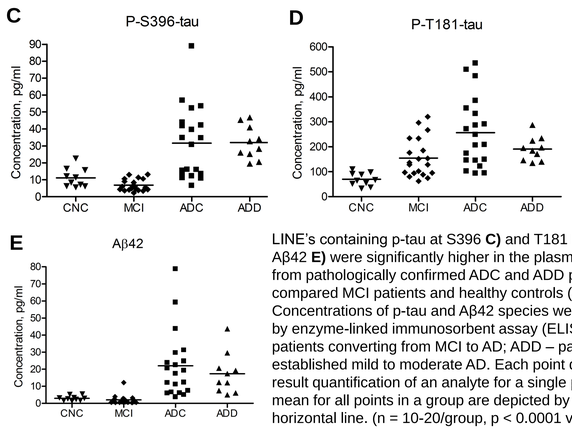

LINE's containing p-tau at S396 **C)** and T181 **D)** and Aβ42 **E)** were significantly higher in the plasma derived from pathologically confirmed ADC and ADD patients compared MCI patients and healthy controls (CNC). Concentrations of p-tau and Aβ42 species were quantified by enzyme-linked immunosorbent assay (ELISA). ADC – patients converting from MCI to AD; ADD – patients with established mild to moderate AD. Each point depicts the result quantification of an analyte for a single patient. The mean for all points in a group are depicted by the horizontal line. (n = 10-20/group, p < 0.0001 vs. CNC)

LINE's containing p-tau were increased in the brain of AD patients

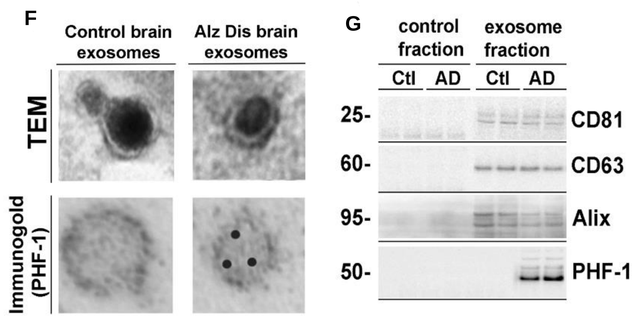

Representative TEM image of L1 – positive exosomes derived from the brains of healthy controls and AD brains **F)**. L1 – positive exosomes contained p-tau as detected by immunogold using the PHF-1 antibody. L1 – positive exosome fractions from healthy controls and AD brains were probed against exosome markers, CD81, CD63, and Alexin and analyzed by immunoblot **G)**. The control fractions (non-exosome, soluble) were negative for all exosome markers while the exosome fractions from the control and AD brains were positive for all three exosome markers. Only the exosome fractions from AD brains were positive for PHF-1 (n = 8/group).

LINE's derived from AD brains seed tau pathology in wild-type mice

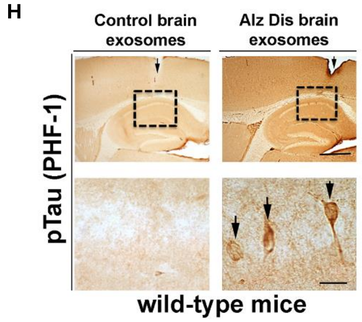

Tau-containing LINE preparations from control and AD brains were injected into the hippocampus of wild-type mice and analyzed 2 months later using immunocytochemistry. **H)** Representative image of hippocampal sections stained with PHF-1. Mice injected with LINEs obtained from AD brains displayed increased PHF-1 immunoreactivity in the CA1 region of the hippocampus (n=8/group).

3R and 4R tau Tg mice develop NFT pathology *in vivo* and shed tau in exosomes

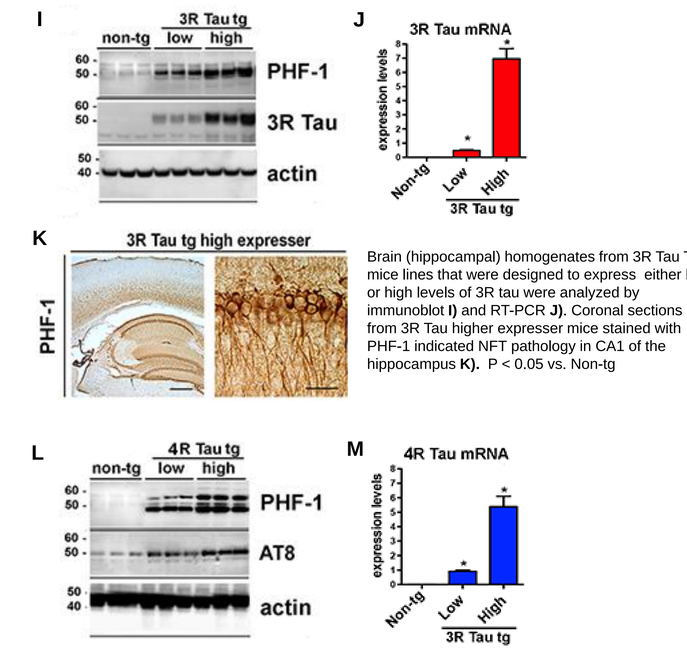

Brain (hippocampal) homogenates from 3R Tau Tg mice lines that were designed to express either low or high levels of 3R tau were analyzed by immunoblot **I)** and RT-PCR **J)**. Coronal sections from 3R Tau higher expresser mice stained with PHF-1 indicated NFT pathology in CA1 of the hippocampus **K).** P < 0.05 vs. Non-tg

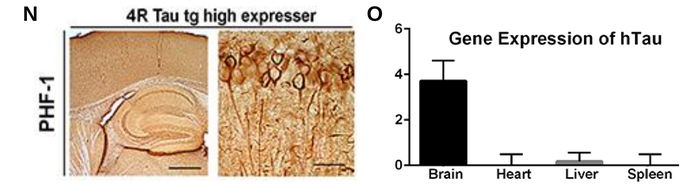

Brain (hippocampal) homogenates from 4R Tau tg mice lines that were designed to express either low or high levels of 4R tau were analyzed by immunoblot **L)** and RT-PCR **M)**. PHF-1 and AT8 immunoreactivity was significantly higher in 4R Tau higher expresser mice. Coronal sections from 4R Tau higher expresser mice stained with PHF-1 indicated NFT pathology in CA1 of the hippocampus **N).** Gene expression as measured by qRT-PCR demonstrated that h-tau is restricted to the brain of 4R **O)** and 3R (data not shown) mice. P < 0.05 vs. Non-tg

Conclusions & Future Directions

Conclusions:

- Tau contained within neuronally-derived exosomes (LINE's) can be feasibly detected in the blood and brain from autopsy-confirmed AD cases
- Tau-containing LINE's can be trafficked at increasing levels from the CNS to the blood as disease severity advances
- Intracerebral injection of tau-containing LINE's derived from AD brains can seed tau pathology in wild-type mice
- The successful isolation and identification of tau-containing LINE's derived from 3R and 4R Tau Tg mice provide a useful animal model to study the trafficking and pathogenicity of LINE's *in vivo*

Future experiments include:

- Assess pathogenicity (neuropathological and behavioral) of LINE's isolated from AD cases and 3R and 4R Tau Tg mice that have been injected into wild-type mice
- Assess pathogenicity of LINE's isolated from paired CSF samples derived from control and AD cases

References:

1. Cleveland, D.W., S.Y. Hwo, and M.W. Kirschner, Purification of tau, a microtubule-associated protein that induces assembly of microtubules from purified tubulin. J Mol Biol, 1977. 116(2): p. 207-25.
2. Kosik, K.S., Tau protein and Alzheimer's disease. Curr Opin Cell Biol, 1990. 2(1): p. 101-4.
3. Goedert, M., Tau protein and the neurofibrillary pathology of Alzheimer's disease. Trends Neurosci, 1993. 16(11): p. 460-5.
4. Medina, M. and J. Avila, Is tau a prion-like protein? J Alzheimers Dis, 2014. 40 Suppl 1: p. S1-3.
5. Chai, X., J.L. Dage, and M. Citron, *Constitutive secretion of tau protein by an unconventional mechanism.* Neurobiol Dis, 2012. 48(3): p. 356-66.
6. Fiandaca, M.S., et al., Identification of preclinical Alzheimer's disease by a profile of pathogenic proteins in neurally derived blood exosomes: A case-control study. Alzheimers Dement, 2014.

Career Development in the Neuropathology of AD:
A novel high-throughput parcellation brain banking protocol

Maxim Signaevski, MD-PhD[1,2,3,4,5], John F. Crary, MD-PhD[1,2,3,4,5], Dushyant Purohit, MD[1,2,3,4,5,6,7], Ann C. McKee, MD[8], Jean-Paul Vonsattel, MD[9], Mary Sano, PhD[3,4,5,6,7]

[1]Department of Pathology, [2]Department of Neuroscience, [3]Friedman Brain Institute, [4]Alzheimer's Disease Research Center, [5]Ronald M. Loeb Center for Alzheimer's Disease and [6]Department of Psychiatry, [7]James J Peters VAMC, Bronx, NY; [8]Department of Neurology, Pathology, Alzheimer's Disease Center, CTE Program, Boston University School of Medicine, VA Boston Healthcare System; [9]Department of Pathology and Cell Biology and the Taub Institute for Research on Alzheimer's Disease and the Aging Brain, Columbia University Medical Center

+ Marco, + ...

ABSTRACT

Alzheimer disease (AD) and related dementias remain a critical problem. Alzheimer Disease Research Center (ADRC) neuropathology cores play a vital role in the research effort, but are limited by a shortage of neuropathologists with the necessary training. The role of a neuropathology core director requires expertise in multiple areas. First, directors must have the ability to diagnose and characterize neurodegenerative brain specimens, integrating histopathological, clinical and molecular findings. They must have the competence to procure, manage and allocate tissue samples for complex multimodality research to maximize the utility of precious resources. Finally, they must be able to develop innovative concepts by applying modern molecular techniques to the evaluation of neurodegeneration.

Specific aims of this training are:

1) to gain advanced training in the neuropathologic evaluation of AD and related neurodegenerative disease by evaluating cases under the guidance of three ADRC neuropathology core directors who will provide focused training in the diagnostic protocols used at each center, supplemented by case-based learning and directed literature reviews;

2) to develop proficiency in managing and maintaining a large dementia brain biorepository via hands-on training under the guidance of three highly experienced ADRC NP core directors; and

3) to examine regional and temporal variation in *MAPT* mRNA isoforms using a novel RNA *in situ* hybridization platform to test the hypothesis that these differences in tau expression drive neurodegeneration.

A novel high-throughput brain banking protocol

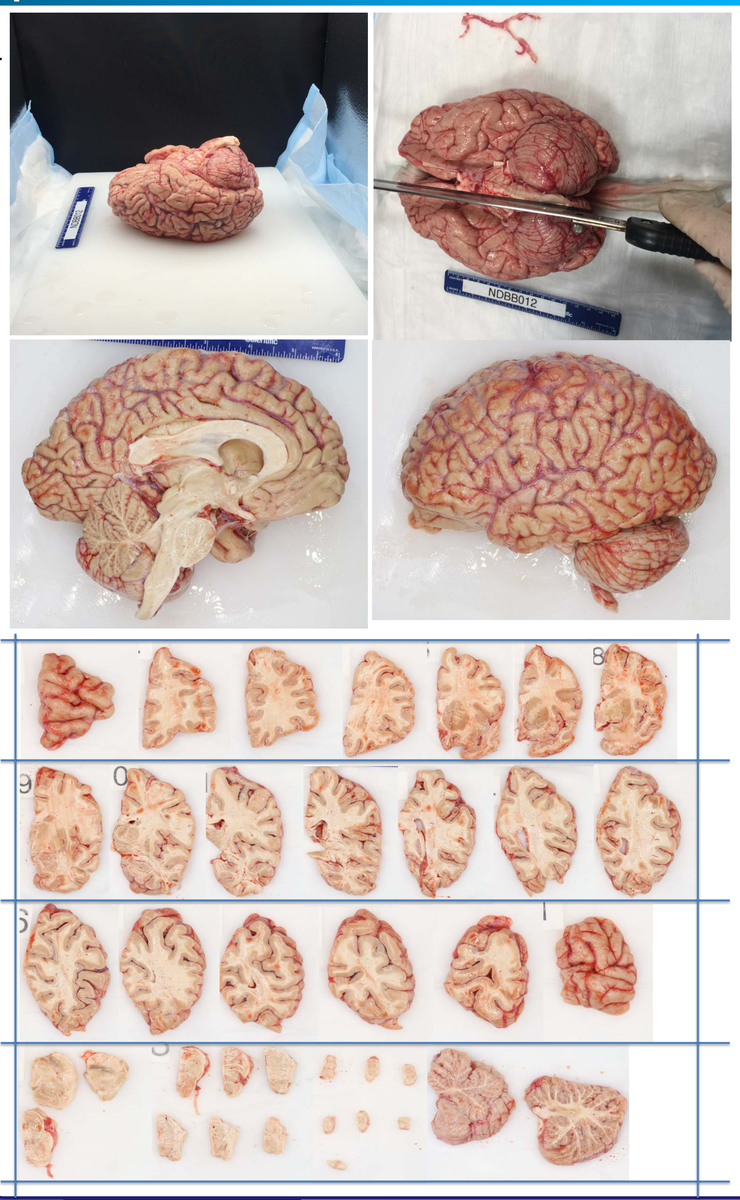

Dissection, barcoding, and annotations

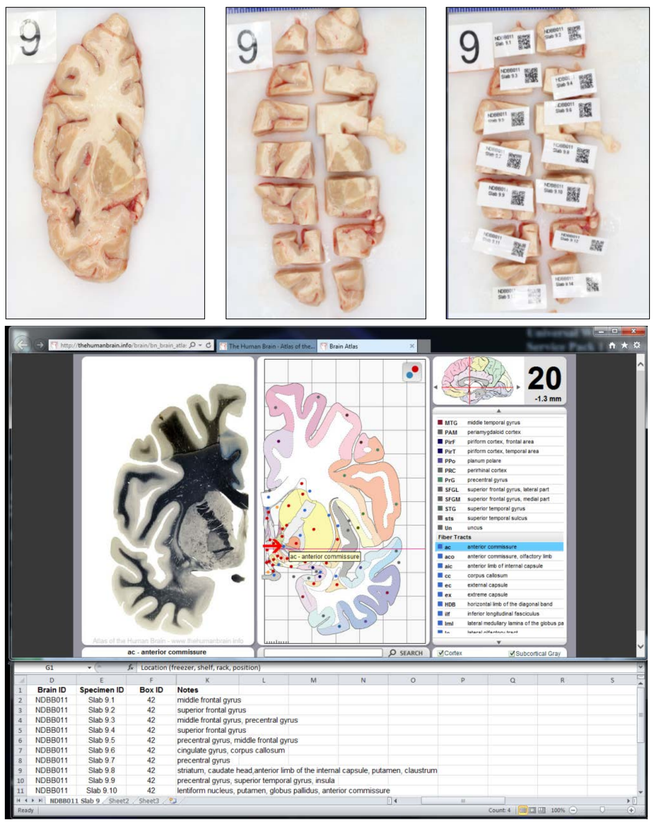

Frozen tissue accessioning

- Barcoded pieces are accessioned in MSSM Freezer Farm
- Records are kept in the Database
- Together with the detailed annotations this allows accessibility to the research community and fast filling the request time

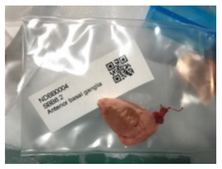

Frozen tissue quality contol

- H&E for tissue integrity and quality of freezing
- pH of the tissue
- Samples are taken for further DNA and RNA analysis

Fixed brain

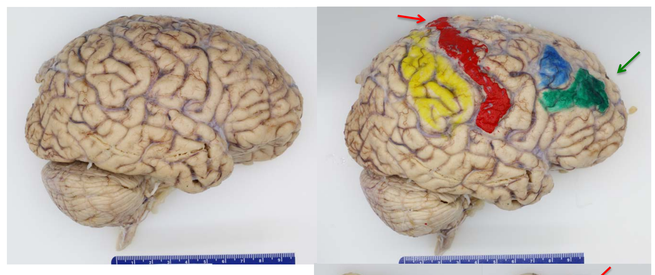

The opposite hemisphere is submersed in 10% neutral buffered formalin. After 2 weeks, the fixed brain is systematically sampled. Sampled brain regions include the frontal cortex (BA9), parietal cortex, primary motor cortex (BA4) etc. according to the modified protocol (Vonsattel *et. al., 2008*)

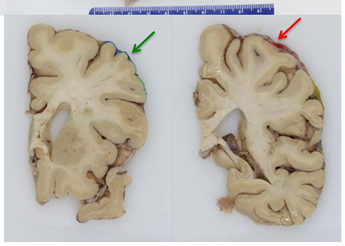

In addition to the routine sampling we use pre-cutting inking of high value areas for the ease of the orientation

Histopathology, IHC, and ISH:

Luxol fast blue/H&E

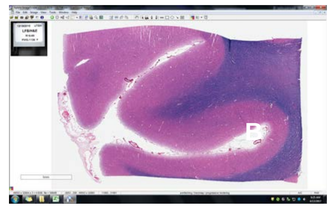

Luxol fast blue/H&E

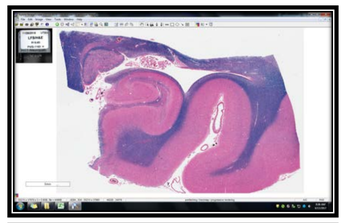

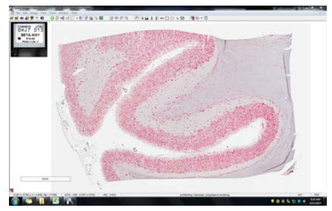

Beta-Amyloid IHC

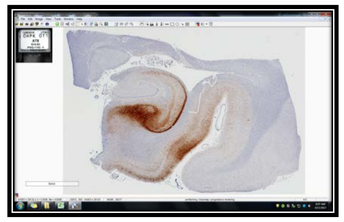

phospho-*tau* IHC

The resulting sections are assessed using a battery of histological (i.e., hematoxylin and eosin/Luxol fast blue and Bielschowsky silver stain) and immunohistochemical (i.e., antisera targeting beta-amyloid, phospho-tau, alpha-synuclein, TDP-43, and ubiquitin) approaches.

Slides are further scanned (Aperio), and regional quantification is performed using proprietary software.

Goals

1. Advanced training in neuropathological evaluation in Alzheimer and related neurodegenerative diseases

On site training at Boston University (Dr. Ann McKee), Mount Sinai (Drs. John Crary, Patrick Hoff, Dushyant Purohit & Susan Morgello), and Columbia University (Dr. Jean-Paul Vonsattel)

2. Proficiency in managing and maintaining a large brain biorepository with the focus in neurodegenerative diseases

3. Maintain research projects :
   - Traumatic brain injury and CTE
   - Regional and temporal variation of tau isoforms in various neurodegenerative conditions

MSSM Neurodegenerative Brain Bank goals and directions

- Establish, develop, and maintain the state-of-the-art brain banking
- Accession up to a 100 brains per year
- Provide a platform for a multidisciplinary research locally and nationally
- Training facility for Brain Bank directors and trainees of all levels

ACKNOWLEDGEMENTS and Grant

We would like to thank all the involved staff at Mount Sinai, Boston University, Columbia University, and James J Peters VAMC, Bronx.

This supplement is funded by NIH-NOA 3P50AG005138-33S2; under 3P50AG005138-33 (Mary Sano)

Multiplexed immunofluorescence for the study of neurodegenerative dementia

Salvatore Spina[1], Dan E. Meyer[2], Alberto Santamaria-Pang[2], Jersey Deng[1], Jesse Brown[1], Sarat Vatsavayai[1], Stephanie Gaus[1], Alissa Nana Li[1], Norbert Lee[1], Ji-Hye Hwang[1], Bruce L. Miller[1], Lea Grinberg[1], William W. Seeley[1,3]

Memory and Aging Center, Department of Neurology[1] and Pathology[3], University of California, San Francisco. [2]GE Global Research, Niskayuna NY

Background

- Confocal immunofluorescence microscopy allows for the contextual visualization of a small number of different markers within a narrow field of view. Important biological relationships such as those between specific cell subtypes, subcellular compartments and various pathological findings must be inferred through examination of multiple histological levels in serial sections.
- We have developed a multiplexed immunofluorescence platform that allows for deep in situ visualization and automated quantification of dozens of molecular markers in the very same formalin-fixed paraffin-embedded histological section.
- We display the results of our preliminary studies assessing a small cohort of primary tauopathy cases and normal controls.

Methods

- 20 tauopathy cases (9 PSP, 6 CBD, and 5 Pick's disease), and 3 controls
- Regions examined: anterior cingulate, inferior frontal, insular, pre-central, post-central and angular cortices, putamen, globus pallidus, amygdala, substantia nigra, tectum, periaqueductal gray
- Markers:
  - i) cell type and subcellular compartment identity (DAPI, NeuN, MAP2, SMI31, SMI32, GFAP, MBP, CNPase, VMAT2, Vimentin, Collagen IV, Iba1, Parvalbumin, Calbindin, Calretinin);
  - ii) tau post-translational modifications and isoforms (AT8, TauC3, TauAcet274, Tau3R and Tau4R);
  - iii) cell death pathway and autophagy (Casp 6 and LC3B);
  - iv) inflammation (C3 and CD68);
  - v) synapses (Spinophilin, PSD95, Synaptophysin);
  - vi) other proteinopathies (Abeta, p62, TDP-43, TDP-43, α-synuclein)

Multiplexed analysis of proteins and DNA in a single formalin-fixed paraffin-embedded slide

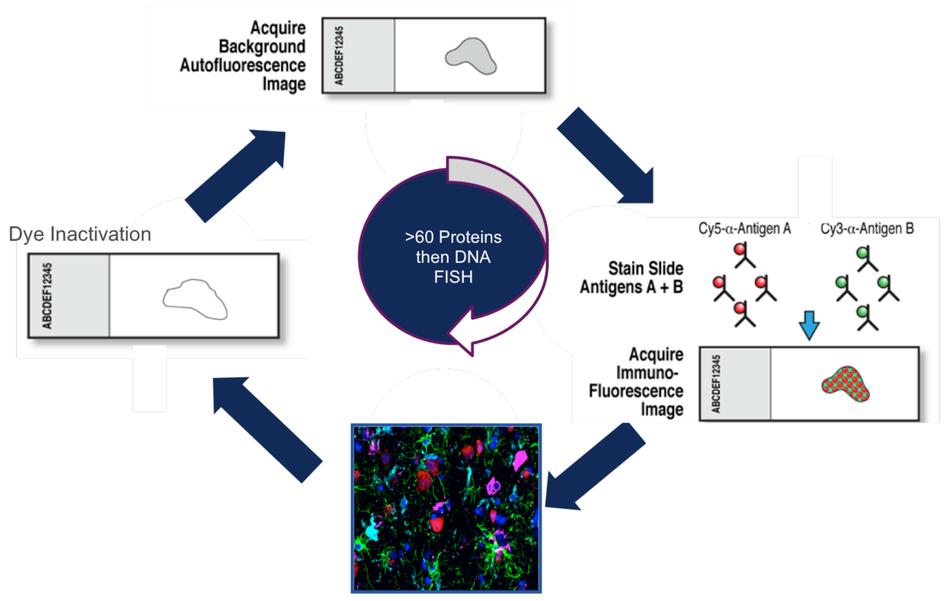

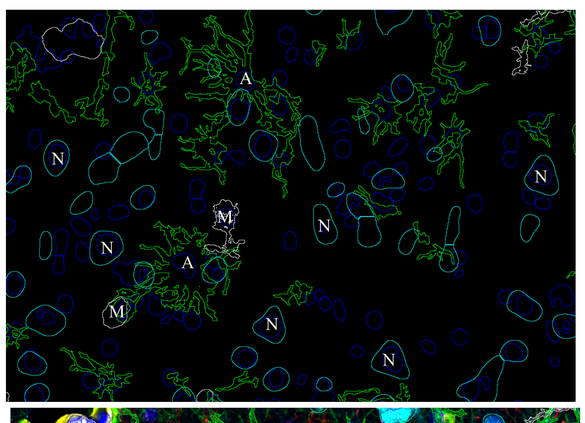

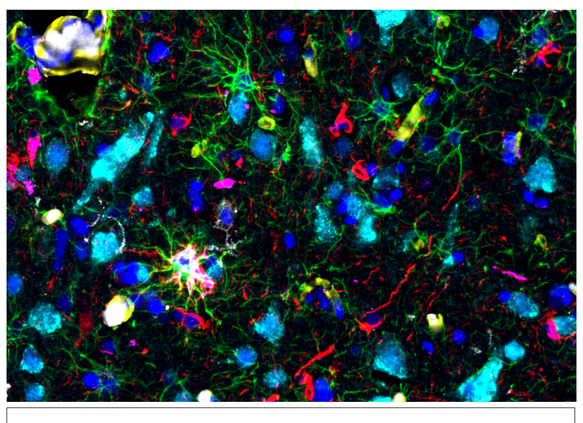

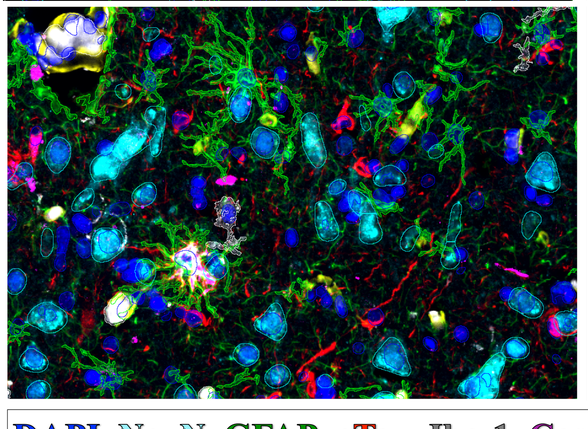

Tissue segmentation and cell type classification are implemented with the use of a machine-learning algorithm on the basis of morphometric data and immunofluorescence signal.

On the top left panel, an example of cell type classification: N = neurons, A = astrocytes, M = microglia cells.

DAPI, NeuN, GFAP, pTau, Iba-1, Caspase 6, Vimentin

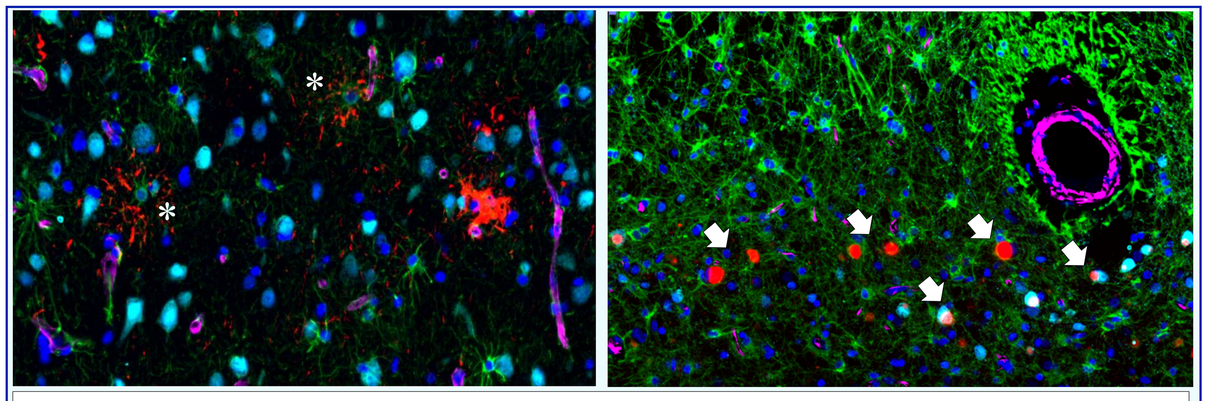

GFAP, pTau, DAPI, NeuN, Vimentin
Astrocytic plaques (left, *) and Pick's bodies (right, ⇨)

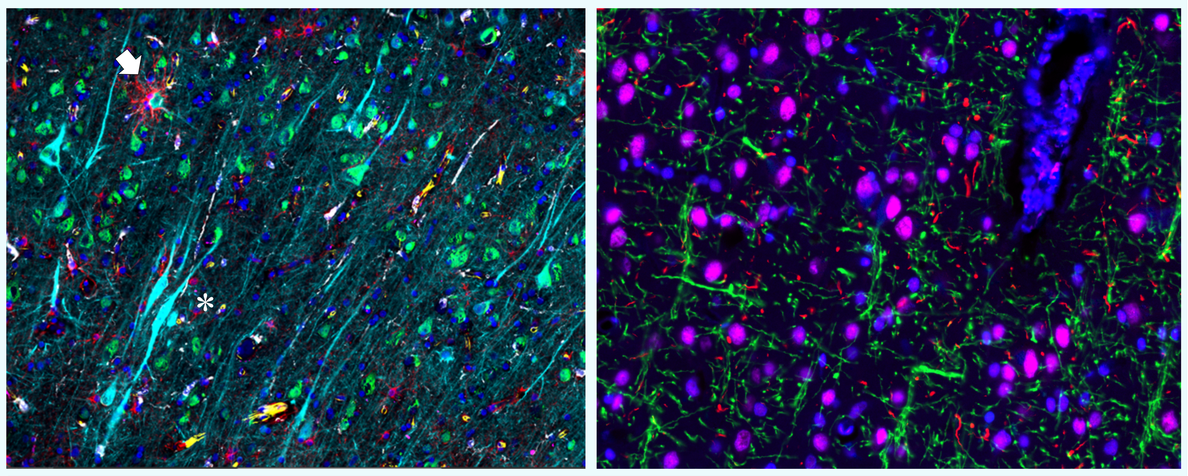

Left = NeuN, pTau, DAPI, VMAT2, Iba-1, Caspase 6, Vimentin, * = Von Economo neurons, ⇨ = tufted astrocyte. **Right = DAPI, pTau, TDP-43, MBP**

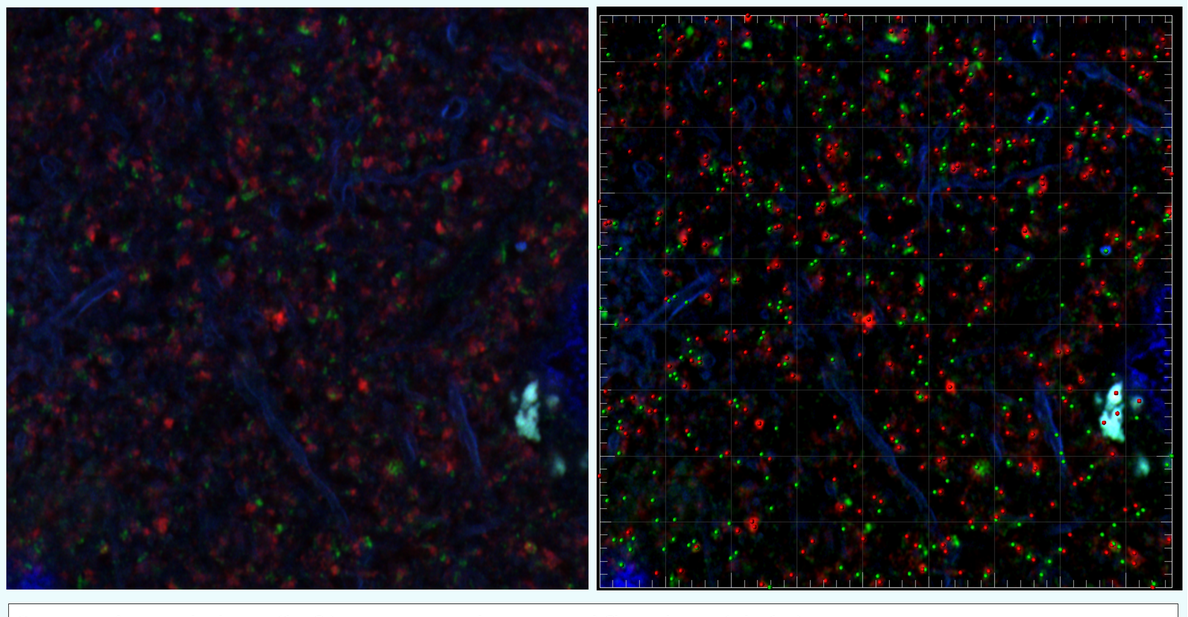

Synaptic staining (left) automatic quantification (right)
Synaptophysin, Spinophilin, confocal Airyscan microscopy

Acknowledgement: This work is supported by the National Institute on Aging grants K08AG052648, P50AG023501 and PO1AG019724, and the Tau Consortium.

ZCCHC17 impairment is a significant driver of neuronal dysfunction in Alzheimer's disease

Zeljko Tomljanovic [1,2], Mitesh Patel [4], Eleni-Konstantina Argyrousi [1,2], William Shin [3], Andrea Califano [3], Andrew F. Teich [1,2]

[1] Columbia University, Department of Pathology and Cell Biology, New York NY, [2] Columbia University, Taub Institute for research on Alzheimer's Disease and the Aging Brain, New York NY, [3] Columbia University Department of Systems Biology, New York NY, [4] Memorial Sloan Kettering Cancer Center, New York NY

Summary

1) We have used bioinformatic tools to investigate potential master regulators of gene expression in the central nervous system that may be disrupted in Alzheimer's disease (1).

2) We have identified a protein, called ZCCHC17, that is predicted to have impaired function in Alzheimer's disease, leading to disruption of synaptic function. ZCCHC17 contains a zinc-finger (CCHC) domain and a nuclear localization signal (2,3), and is not well studied, although it has been previously linked to AD (4).

3) We have determined that ZCCHC17 protein (I) Is localized to neuronal nucleoli in the CNS, (II) Is decreased in Alzheimer's disease tissue, (III) directly or indirectly regulates gene expression of 60% of its predicted synaptic targets in rodent neuronal cultures, and (IV) ZCCHC17 knock-down impairs expression of genes in several synaptic ontology groups, impairs potassium currents, and lowers the action potential threshold.

4) These data support the hypothesis that ZCCHC17 supports normal synaptic function and that ZCCHC17 impairment contributes to synaptic dysfunction in AD.

Computational Analysis

ZCCHC17 impairment is predicted to drive synaptic dysfunction in AD. We used computational tools that predict master regulators (MRs) that drive changes in gene expression in a disease state, and applied them to AD (1). A Synaptic Score (S_{MR}) value was generated for each master regulator, which is essentially a sum of the change in a MR's synaptic targets in AD, weighted by the correlations between the MR and each target. MRs with large negative S_{MR} values have large positive correlations with synaptic genes with large decreases in expression in AD.

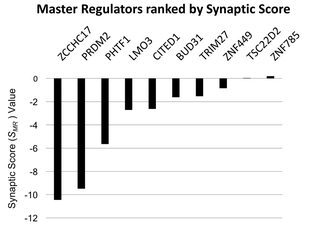

Shown to the left are the top 10 master regulators in our analysis with the most negative S_{MR} values. ZCCHC17 has the most negative value in our analysis, which suggests that ZCCHC17 1) Normally supports the expression of a large number of synaptic genes, and 2) ZCCHC17 dysfunction contributes to synaptic dysfunction in AD.

Molecular Analysis

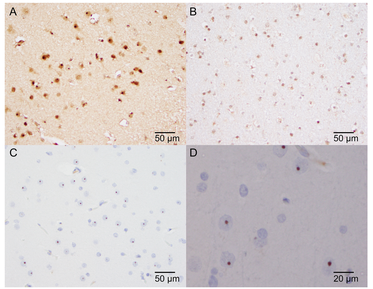

ZCCHC17 is expressed in several cell types, but is most strongly expressed in neurons. Immunohistochemistry was performed for ZCCHC17. At high antibody concentrations, anti-ZCCHC17 antibody stains nuclei strongly and cytoplasm weakly in grey matter (panel A), and nuclei weakly in white matter (panel B). At lower antibody concentrations, anti-ZCCHC17 selectively stains the nucleoli of large neurons in grey matter, as shown in panel C (low magnification) and panel D (high magnification).

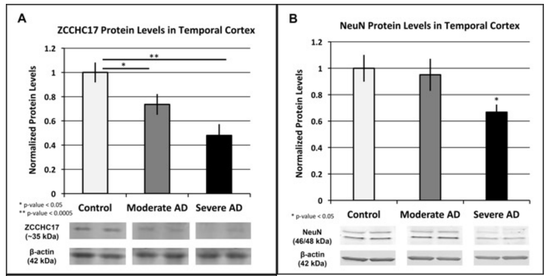

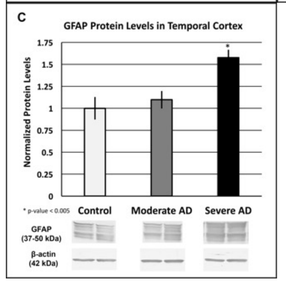

ZCCHC17 is lost at early stages of AD, before significant gliosis and neuronal loss. (A) ZCCHC17 shows statistically significant changes in both moderate AD and severe AD in temporal cortex. This is before significant neuronal loss (as measured by NeuN, panel **B**) or astrogliosis (as measured by GFAP, panel **C**). All bands are normalized by beta-actin; n = 9 for control, 10 for moderate AD, and 10 for severe AD.

ZCCHC17 knock-down leads to reduced expression of three of its predicted synaptic targets. After ZCCHC17 knock-down, three of ZCCHC17's predicted synaptic targets were selected based on particularly strong positive Spearman's correlation coefficients in our computational work. All three targets (Synaptotagmin 1, Synapsin 2, and Synaptic Vesicle Protein 2B) showed a statistically significant reduction using qPCR after ZCCHC17 knock-down. Subsequent RNA-seq has shown that 60% of the synaptic genes predicted to be driven by ZCCHC17 in human neurons are decreased in rat neuronal cultures after ZCCHC17 knock-down.

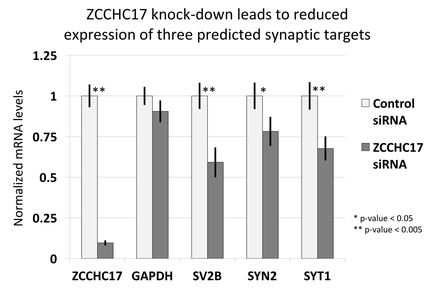

ZCCHC17 has a relatively conserved function across species. Our human interactome work predicts the relationship of genes with ZCCHC17 in our rat data. Every gene that is linked to ZCCHC17 through our interactome analysis (which uses human data) and that also has a significant correlation with ZCCHC17 in our rat data is represented by a point. For each gene, the x-axis displays the human interactome-derived Spearman's correlation of a given gene with ZCCHC17. The y-axis displays the Spearman's correlation of a given gene with ZCCHC17 as derived from our rat data. Genes with strong positive correlations or strong negative correlations in both humans and rats are colored blue; genes with discordant correlations (positive in one species, negative in another) are colored black. Note that for genes that positively correlate with ZCCHC17 in our human data (right half), more reach positive significant correlations with ZCCHC17 in our rat data (157 genes; blue dots upper right quadrant) than reach negative significant correlations in our rat data (34 genes; black dots lower right quadrant). The same relationship holds for the minority of genes predicted to negatively correlate with ZCCHC17 in our human data (i.e. there are more blue dots in lower left quadrant (19 genes) than black dots in the upper left quadrant (7 genes)). Overall, 81% of the genes that reach significance in the rat data have the same sign of correlation in the human data (p-value < $2.2 * 10^{-16}$, binomial test).

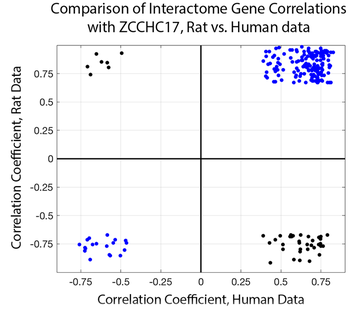

Physiology

A Ontology Analysis of ZCCHC17 knock-down: ontology category name	z-score
Transmission across Chemical Synapses	-5.81
Potassium Channels	-5.67
Cholesterol biosynthesis	-5.44
Neurotransmitter Receptor Binding And Downstream Transmission In The Postsynaptic Cell	-4.80
Voltage gated Potassium channels	-4.62
Neurotransmitter Release Cycle	-3.75
Norepinephrine Neurotransmitter Release Cycle	-3.65
CRMPs in Sema3A signaling	-3.65
CaM pathway	-3.55
Calmodulin induced events	-3.55

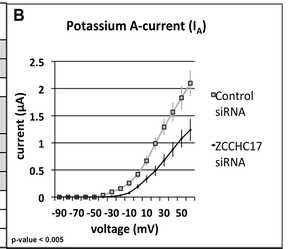

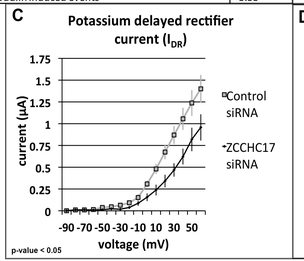

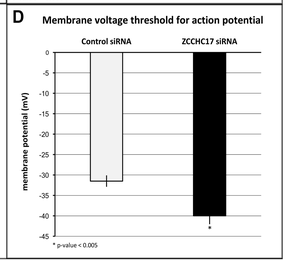

ZCCHC17 knock-down leads to impaired potassium currents. (A) ZCCHC17 knock-down is characterized by impaired expression of ontology groups related to synaptic function. Shown here are the top 10 most significant categories, which are all characterized by a net decrease in gene expression (see negative Z values). Six of these categories (shaded in grey) relate to synaptic function. Of note, two of the categories relate to potassium function. **(B-D)** Potassium currents are reduced after ZCCHC17 knock-down, and are associated with a lower action potential threshold. In (D), we measured the lowest voltage step that produced an action potential for each cell, and compared control vs. ZCCHC17 siRNA groups. ZCCHC17 knock-down leads to a statistically significant decrease in the action potential threshold.

References

1) Aubry, S., et al, PLoS One, 10(3), e0120352, 2015
2) Gueydan, C., et al., J. Biol. Chem., 277(47), 45034-40, 2002
3) Chang, W. L., et al., Biochem. Biophys. Res. Commun., 307(3), 569-77, 2003
4) Li, X, et al., Sci Rep, 2015. 5:12393.

Primary Age-Related Tauopathy Working Group Study: Quantification and distribution of neuropathologic changes in PART

Jamie M. Walker[1,2], Kurt Farrell[3], Timothy E. Richardson[4], Eileen H. Bigio[1,2], Charles L. White III[4] and John F. Crary[3]

Department of Pathology[1], Northwestern University Feinberg School of Medicine, Northwestern University Cognitive Neurology and Alzheimer Disease Center[2], Chicago, IL; Department of Pathology, Icahn School of Medicine at Mount Sinai[3], New York, NY; Department of Pathology, UT Southwestern Medical Center[4], Dallas, TX

Introduction

Primary Age-Related Tauopathy (PART) is a neurodegenerative disorder characterized by symptoms of dementia with an older age of death than Alzheimer disease, and usually a milder amnestic dementia (1). Histopathologic changes in PART are primarily restricted to Braak stage I-IV, and Thal phase 0-2 (2). Historically, some of the most severely affected subjects have been categorized as tangle-predominant senile dementia or tangle-only dementia (3,4). There is some debate as to whether PART has a distinct pathogenesis, or rather is simply a precursor or subset of AD (5,6). The objective of this project is to test the working hypothesis that PART cases have distinct clinical, genetic and neuropathologic characteristics that distinguish them from AD and other neurodegenerative disorders. The rationale is that distinguishing these disorders will give us insight into the mechanisms of tau and amyloid deposition and degradation, and will allow clinicians to formulate more specific and accurate diagnoses, which will eventually lead to more specific therapeutic modalities.

Research Objectives

Aim 1: Develop quantitative measures of tau pathology in PART

- Develop a standardized method to quantitate neurofibrillary tau pathology in a given region, that will lead to reliable and reproducible results by all observers
- Operationalize the currently proposed diagnostic criteria and reach a consensus diagnosis for cases in the study

Aim 2: Correlate quantitative and qualitative histopathologic findings in PART with clinical, genetic and biochemical data

- Correlate severity of PART neuropathologic changes with clinical severity of dementia
- If genetic studies link specific genetic variations to PART cases, then it would be plausible to test whether these genes play a role in the mechanism of PART resistance to amyloid deposition, or promotion of amyloid degradation

Methods

Cases (n~1200)

- Tissues and existing data have been collected from neurodegenerative disease brain bank cases that meet the new neuropathologic criteria for possible or definite PART, and Braak 0 controls (see Table 1. for inclusion/exclusion criteria)
- Assembling a cohort of ~1000 pure PART subjects from over 30 centers that span the ages of 50-110+ for genetic, biochemical and neuropathological studies (see Table 2. for an overview of the current cohort)

Phase I

- LFB/H&E staining will be performed on frontal and hippocampal sections from each case
- Frontal sections will be immunostained for β-amyloid
- Hippocampal sections will be immunostained for p-tau

Phase II

- If frontal section is positive for beta-amyloid, it will be immunostained for p-tau to rule out tau-postive neuritic plaques, and the hippocampal section will be immunostained for β-amyloid to help determine the Thal phase

Phase III

- If necessary, Hirano stains will be performed on sections to help identify neuritic plaques
- Select sections will be stained with 3R and 4R-tau immunostains

Sections evaluated using immunostains for:

- Phosphorylated-tau (AT8)
- β-amyloid (6E10, monoclonal to residues 1-16, BioLegend)

All stained slides will be scanned into the Aperio system at UT Southwestern

- Semiquantitative and quantitative analysis of temporal lobe tau burden using imaging software

Clinical and Pathologic Findings

Table 1. PART study case inclusion/exclusion criteria

Clinical History		Neuropathology	
Age	50-110+	Neurofibrillary tangles	Any Braak stage, controls (Braak 0)
Diagnosis	No dementia, MCI, dementia	Amyloid plaques	CERAD score: none or sparse
Other	M or F	Other	Vascular, LBs and abnormal TDP-43 acceptable
Exclusions	MND, movement disorders, FTD	Exclusions	Other NFT diseases (FTLD-tau; PSP/CBD, Pick, GGT, etc.)

Table 2. Current cohort

Braak NFT stage		Gender		CERAD plaque Score		Average age, years (range)	Clinical dementia status		
		Male	Female	*None*	*Sparse*		Normal	MCI	Dementia
0	118	76	42	111	7	72.56, (50-104)	68	19	20
I	148	84	64	121	27	78.5, (56-108)	109	17	18
II	195	95	100	159	36	83.7, (56-108)	115	39	32
III	158	57	101	133	25	90.72, (68-108)	94	25	33
IV	114	38	76	77	38	91.49, (67-106)	40	23	48

Table 3. Contributing institutions

Contributing Institutions			
Northwestern University	Emory University	University of Ulm	Mass General Hospital
Uppsala University	University of Kentucky	Kanazawa University	New York University
Washington University Saint Louis	Banner Sun Health Research Institute	Tokyo Metropolitan Geriatric Hospital	University of Southern California
Icahn School of Medicine at Mt. Sinai	University of Pittsburgh Medical Center	University of California San Francisco	Johns Hopkins Medical Institute
Rush University	University of Texas Southwestern	University of Geneva	Mayo Clinic
Newcastle University	Boston University	University of Pennsylvania	University of Washington
Medical University of Vienna	Oregon Health Science University	Columbia University	University of British Columbia
Indiana University	University of California Los Angeles	University of California Irvine	University of California San Diego

Figure 1. Sample of Aperio scanned images (AT8 stained hippocampal sections)

Figure 2. Aperio image analysis, quantification of tau burden

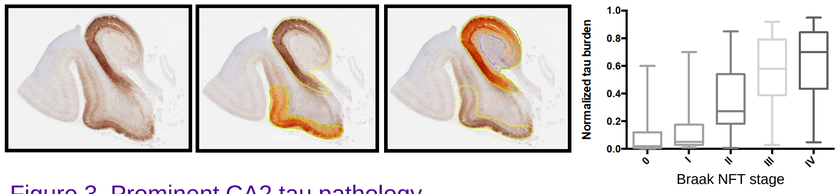

Figure 3. Prominent CA2 tau pathology

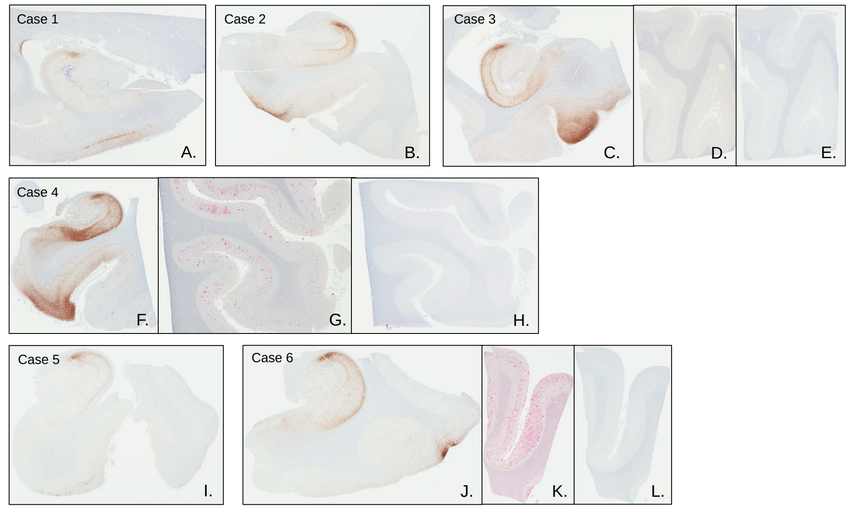

Case 1 and 2: AT8 Braak III, frontal β-amyloid negative (A & B), Case 3: AT8 Braak III, minimal frontal β-amyloid, frontal AT8 negative (C, D & E), Case 4: AT8 Braak III, frontal β-amyloid positive, frontal AT8 negative (F, G & H), Case 5: AT8 Braak III, frontal β-amyloid negative (I) and Case 6: AT8 Braak III, frontal β-amyloid positive, frontal AT8 negative (J, K & L).

Preliminary Findings and Future Directions

- Continue with staining, scanning and analysis of cases
  - Establish whether or not PART cases have *significant* CA2 regional vulnerability for tau pathology that would distinguish them from AD cases
- GWAS on all PART cases, ongoing at Genentech (Gai Ayalon, PhD)
  - If certain genetic variations are found to be associated with PART cases, discover the mechanism by which these variations could lead to increased degradation, or resistance to production of amyloid and neuritic plaques
- Biochemical analysis of amyloid isoforms in PART cases, ongoing at Mt. Sinai

References

1) Crary JF. Primary age-related tauopathy and the amyloid cascade hypothesis: the exception that proves the rule? J Neurol Neuromedicine 1(6):53-57;2016
2) Crary JF et al. Primary age- related tauopthy (PART): a common pathology associated with human aging. Acta Neuropathol 128(6):755-66;2014
3) Jellinger KA et al. PART, a distinct tauopathy, different from classical sporadic Alzheimer disease. Acta Neuropathol 129(5):757-62;2015
4) Jellinger KA, Attems J. Neurofibrillary tangle-predominant dementia: comparison with classical Alzheimer disease. Acta neuropathol 113(2):107–17;2007
5) Duyckaerts C et al. PART is part of Alzheimer disease. Acta Neuropathol 129(5):749-56;2015
6) Braak H, Del Tredici K. Are cases with tau pathology occurring in the absence of Abeta deposits part of the AD-related pathological process? Acta neuropathol 128(6):767–72;2014

Acknowledgements

The authors would like to thank Ping Shang and Jeff Harris for their exceptional staining of the cases, Chan Foong for taking time to scan the cases and for his technical assistance, Niccole Williams for her excellent administrative assistance, graduate students at Mt. Sinai for their continuing work on the project and collaborators at Genentech for the ongoing genetic analyses. Funding provided by the UT Southwestern, Mt. Sinai and Northwestern ADRC grants, as well as the PART R01 (R01NS095252).